Middle Campanian (Late Cretaceous) sea-level rise; microfossil record of bathymetric changes

MICHAŁ FĄFARA[1]*, ZOFIA DUBICKA[1], MARIUSZ NIECHWEDOWICZ[1], AGNIESZKA CIUREJ[2]
and IRENEUSZ WALASZCZYK[1]

[1] *University of Warsaw, Faculty of Geology, Żwirki i Wigury 93, 02-089 Warszawa, Poland.*
[2] *Department of Geology and Palaeontology, Institute of Biology and Earth Sciences, Pedagogical University
of Kraków, Podchorążych 2, 30-084 Kraków, Poland.*
* Corresponding author: m.fafara@student.uw.edu.pl

ABSTRACT:

Fąfara, M., Dubicka, Z., Niechwedowicz, M., Ciurej, A. and Walaszczyk, I. 2023. Middle Campanian (Late Cretaceous) sea-level rise; microfossil record of bathymetric changes. *Acta Geologica Polonica*, **73** (4), 661–683. Warszawa.

A Middle Campanian (Late Cretaceous) eustatic sea-level rise recorded in the Belgorod succession (Russia; eastern North European Basin) was analyzed. The succession, dated for the *Gavelinella annae* and *Globorotalites emdyensis* foraminiferal zones (corresponding to the '*Inoceramus*' *azerbaydjanensis*–'*Inoceramus*' *vorhelmensis* inoceramid Zone), records the deposition of pure chalk, with only trace terrigenous material. Its distal offshore position limited terrestrial nutrient delivery, driving oligotrophic conditions that influenced benthic foraminifera and organic-walled phytoplankton communities. Eustatic changes are recorded by planktonic foraminifera and additionally reflected in phytoclast abundance, organic-walled dinoflagellate cysts (dinocysts), calcareous dinoflagellate cysts (c-dinocysts), and $\delta^{13}C$ and $\delta^{18}O$ fluctuations. Most indices were primarily driven by variable terrestrial organic matter and freshwater influxes, acting as a function of sea depth and land topography.

Key words: Foraminifera; C-dinocysts; Dinoflagellata; Phytoclasts; Chalk.

INTRODUCTION

Microfossils are powerful paleoenvironmental tools, providing information about many paleoceanographic parameters, including – but not limited to – water depth, temperature, salinity, primary productivity, and trophic conditions (Schmiedl 2019). Microfossil paleoenvironmental proxies can be generally divided into two types: (1) those based on assemblage structure (e.g., diversity parameters, test morphotypes); and (2) those based on geochemical indices (such as trace element and isotopic compositions) derived from microfossil shells.

Of the microfossil groups treated in this study, planktonic foraminifera are potentially useful in examining bathymetric changes, especially in relatively shallow seas, whereas benthic foraminifera are sensitive to sea floor oxygen concentrations and organic matter inputs (Jorissen *et al.* 1995; Van der Zwann *et al.* 1999; Friedrich 2010; Dubicka *et al.* 2014; Avnaim-Katav 2020). In turn, dinoflagellate cysts including organic walled and calcareous cysts (c-dinocysts; Ciurej *et al.* 2023) are good proxies for estimating surface temperature, surface salinity, relative sea-level change, nutrient abundance and upwelling strength (e.g., Powell *et al.* 1992; Brinkhuis 1994; Prauss 2000; Pross and Brinkhuis 2005; Sluijs *et al.* 2005; Zonneveld *et al.* 2013; Ciurej *et al.* 2017; Niechwedowicz *et al.* 2021; Ciurej 2023). Moreover, sedimentary organic matter may additionally contain

Text-fig. 1. Campanian (~75 Ma) paleogeography of Europe (after Blakey 2014); Belgorod is marked by a star.

other palynomorphs (such as acritarchs, freshwater and marine algae, and sporomorphs), terrestrial organic particles (translucent and opaque phytoclasts, cuticles), and amorphous organic matter, which, collectively can serve as reliable tools in assessing (paleo)environmental conditions, in particular relative proximity to the shoreline and bottom-water oxygenation; such analysis is commonly referred to as palynofacies analysis (e.g., Tyson 1993, 1995; Roncaglia and Kuijpers 2006).

The Late Cretaceous captures elevated temperatures and the highest sea-levels known throughout the Mesozoic, resulting in vast, shallow and warm epicontinental seas, with widespread calcium carbonate production (e.g., the Western Interior Seaway, or the European Shelf Sea extending from the Atlantic Ocean to western Asia; Hallam 1992; Miller *et al.* 2005; Gale *et al.* 2008). Several large amplitude oscillations during this global highstand triggered major environmental stresses that significantly affected marine ecosystems.

Three significant global sea-level rises are noted during the Campanian. These highs, marked on the sea-level curve of Hancock (1989) as peaks nos. 1 to 3, are well recognized in north-western Europe (Hancock and Kauffman 1979; Hancock 1993; Niebuhr 1999, 2006) and North America (Hancock 1993).

Of these, the least recognized is peak no. 2, dated for the Middle Campanian (Hancock 1993). The first aim of the present paper is the presentation of the micropaleontological record of a Campanian sea-level rise that seems to correlate with the poorly known Hancock's peak no. 2. This study is based on the Campanian succession of the Belgorod section (central European Russia), representing the east-central part of the North European Cretaceous Basin. The compilation of data on planktonic and benthic foraminiferal assemblages, organic-walled and calcareous dinoflagellate cysts, sedimentary organic matter studies, and $\delta^{13}C$ and $\delta^{18}O$ analyses in selected benthic and planktonic foraminiferal tests, revealed a clear pattern of environmental changes within the early Middle Campanian, which can be interpreted in terms of a response to distinct sea-level rise accompanying the transgressive-regressive pulse of that time.
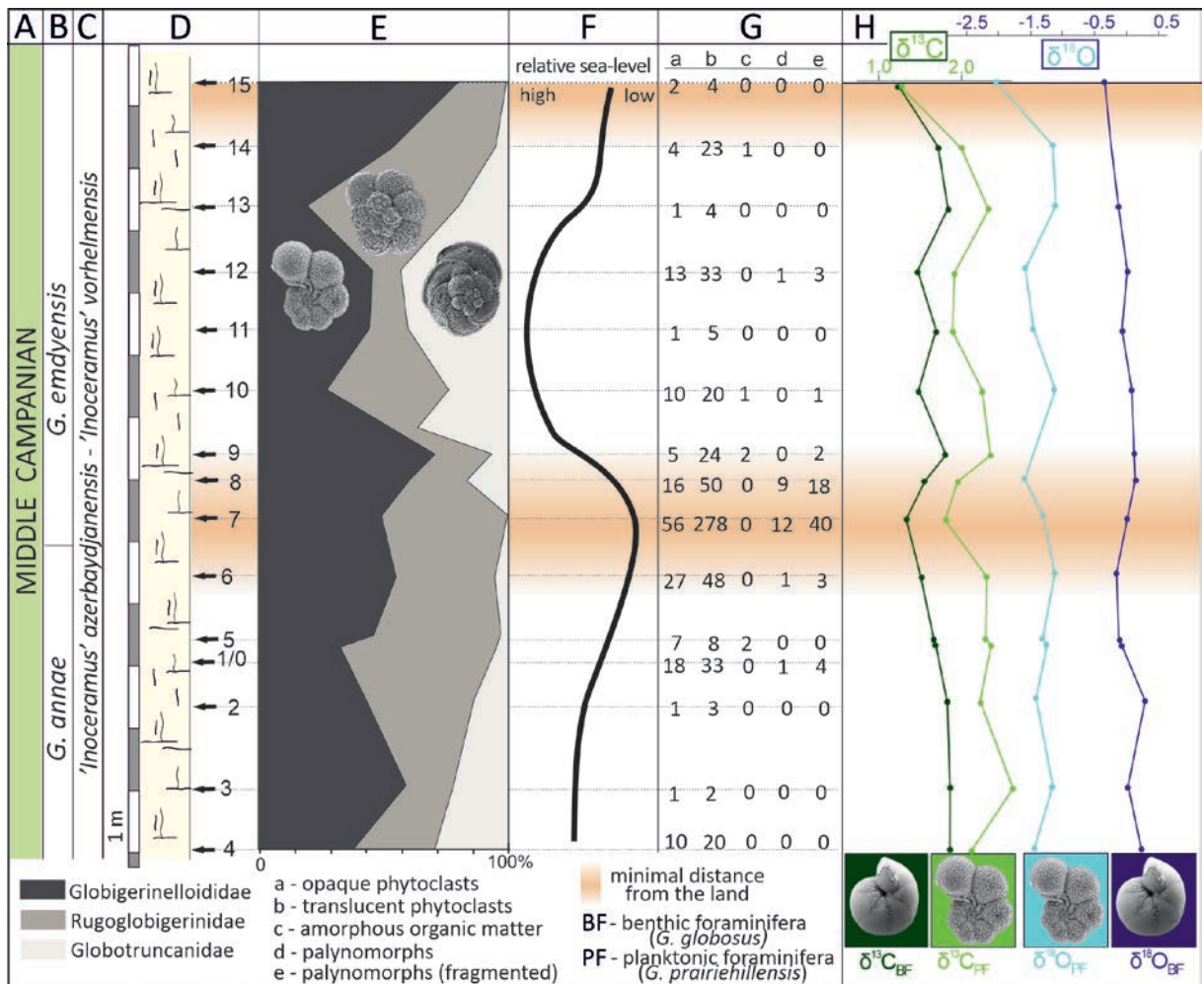
The second aim of this paper is a demonstration of how powerful micropaleontological and geochemical indices, in combination, can be in deciphering environmental changes accompanying the sea-level fluctuations following the transgressive-regressive pulses. The presented discussion contributes to a better understanding of the influence of sea-level changes on paleoceanographic conditions and sedimentology of Cretaceous epicontinental seas.

MATERIALS AND METHODS

Fieldwork was conducted during a field excursion accompanying the Ninth All-Russian Conference (with international participation) *Cretaceous system of Russia and near abroad: problems of stratigraphy and paleogeography* in Belgorod, Russia, organized by Belgorod State National Research University in September 2018 (Baraboshkin *et al.* 2018). Samples for microfossil, palynofacies, and geochemical investigations were collected in the Belgorod chalk mine in central European Russia, approximately 500 km south of Moscow. The Belgorod mine is a huge quarry in the north-western outskirts of the city of Belgorod, structurally located in the south-western margin of the Voronezh Anteclise (e.g., Mushenko 1961; Savko and Ivanova 2009) in the central East European Platform (Text-fig. 1). Campanian strata are well exposed in the northern quarry wall, and are easily accessible over ~1 km along an approximately east-west strike. Samples were collected every meter near the center of the northern wall, capturing a c. 15 m thick succession (Text-fig. 2).

Foraminiferal samples were disintegrated in Glauber's salt ($Na_2SO_4 \times 10H_2O$), cleaned in an ultrasonic bath, and washed through a 100 μm sieve. Up to 250 planktonic and benthic foraminiferal specimens were picked from the obtained residuum under a stereo microscope (see Table A1 in the Appendix 1 at the end of the text). When fewer than 150 planktonic foraminifera were picked, additional extractions were conducted (see Table A2 in the Appendix 1). Foraminiferal

Text-fig. 2. Lithological column of the Belgorod section with the collected results. The columns refer to: (A) Campanian substage division following the tripartite US definition; (B) foraminiferal zonation after Dubicka (2015); (C) inoceramid zonation after Walaszczyk *et al.* (1997, 2016); (D) lithological column; (E) relative abundance of main planktonic foraminiferal morphogroups; (F) sea-level curve of the studied basin; (G) quantitative palynofacies results; and (H) $\delta^{13}C$ (green) and $\delta^{18}O$ (blue) curves for planktonic, i.e., *Globigerinelloides prairiehillensis* Pessagno, 1967 and benthic, i.e., *Gyroidinoides globosus* (Hagenow, 1842) foraminifera, respectively.

Wall type	Pithonelid	Tangential	Radial					Oblique				Diversity of wall type		
Species/ Sample	*Lentodinella danica*	*Fuettererella deflandrei*	*Orthopithonella porata*	*Orthopithonella* aff. *gustafsonii*	*Orthopithonella* sp. A	*Orthopithonella* sp. B	*Orthopithonella* sp. C	*Pirumella edgarii*	*Pirumella cylindrica*	*Pirumella loeblichii*	*Pirumella thayrei*	Radial	Oblique	Species diversity
Bel 15	F	VR		R	F	R		R	F	R	F	3	4	9
Bel 11		VR		VR	VR	VR				VR	VR	3	2	6
Bel 9				VR		VR	VR			VR	VR	3	2	5
Bel 5		R	VR	R			VR	VR	VR	R	R	4	4	8
Bel 3		F	VR	R	R			R		F	R	4	3	7

Table 1. Distribution of calcareous dinocysts in the Belgorod section. Explanations: VR – very rare, R – rare, F – frequent.

assemblage metrics included: (1) relative frequencies of calcareous and agglutinated forms within benthic assemblages; (2) planktonic/benthic (P/B) ratios [the percentage of planktonic foraminifera in the foraminiferal associations, expressed as $100 \times P/(P+B)$]; and (3) the relative proportions of selected benthic genera and planktonic morphotypes. Photographic documentation of stratigraphically important taxa and, prior to isotopic analysis, foraminiferal test preservation was conducted with a Zeiss Σigma VP field emission scanning electron microscope (FE-SEM) at the Faculty of Geology, University of Warsaw.

Five samples were analyzed for calcareous dinocysts (c-dinocysts) (Table 1). Ten g of sediment were disintegrated in Glauber's salt. Obtained residues were cleaned in an ultrasonic bath and sieved into three fractions: <20 μm, 20–75 μm, and 75–125 μm. C-dinocyst specimens were picked from the 20–125 μm fractions, using a standard optical binocular microscope. Taxonomic identification was conducted with a HITACHI 3-4700 scanning electron microscope (SEM) at the Laboratory of Field Scanning Emission Microscopy and Microanalysis at the Institute of Geological Sciences, Jagiellonian University. The specimens were coated with gold and observed under secondary electron mode, with acceleration voltage set to 20 keV under high vacuum and a work distance of approximately 13.0 mm (12.4 to 14.4 mm). For c-dinocyst taxonomic identification, selected morphologic characters – including, but not limited to, shape, size, aperture, and wall ultrastructure – were observed. In particular, wall structure formed the basis for c-dinocyst classification. Four cyst wall ultrastructure styles, based on crystal orientation within the wall, were recognized: pithonellid, radial, oblique, and tangential (Keupp 1987; Kohring 1993; Young *et al.* 1997).

Sedimentary organic matter was extracted from 70 g of dry sediment. The samples were processed using standard palynological preparation techniques (hydrochloric and hydrofluoric acid treatments with repeated decantation, heavy liquid separation). The extracted organic residues were sieved through a 15 μm nylon mesh and concentrated via centrifugation. A drop of macerate obtained from each sample was mounted on a slide using glycerin jelly, and overlain with a 20×20 mm coverslip. Identification and counting of palynomorphs and other kerogen particles was conducted under a transmitted light microscope (three slides per sample were examined). The classification of sedimentary organic matter follows Tyson (1993, 1995); kerogen particles were subdivided into the following categories: (1) opaque phytoclasts (black woody tissue); (2) translucent phytoclasts (brown woody tissue completely translucent to translucent only at the edges); (3) cuticle (leaf tissue); (4) palynomorphs (marine- and terrestrially-derived organic-walled microfossils, such as dinocysts, acritarchs, marine and freshwater algae, foraminiferal organic linings, spores, and non-saccate and saccate pollen grains); and (5) amorphous organic matter (AOM). The palynomorph taxonomy follows Fensome *et al.* (2019). Kerogen particle abundances are given as the number of particles counted per slide.

The investigated foraminifera and organic-walled dinoflagellate cysts are housed at the S.J. Thugutt Geological Museum, Faculty of Geology, University of Warsaw, collection no. MWGUW ZI/67, while the c-dinocysts are housed at the Institute of Biology and Earth Sciences, Pedagogical University of Krakow, collection no. UPKG/1/2023.
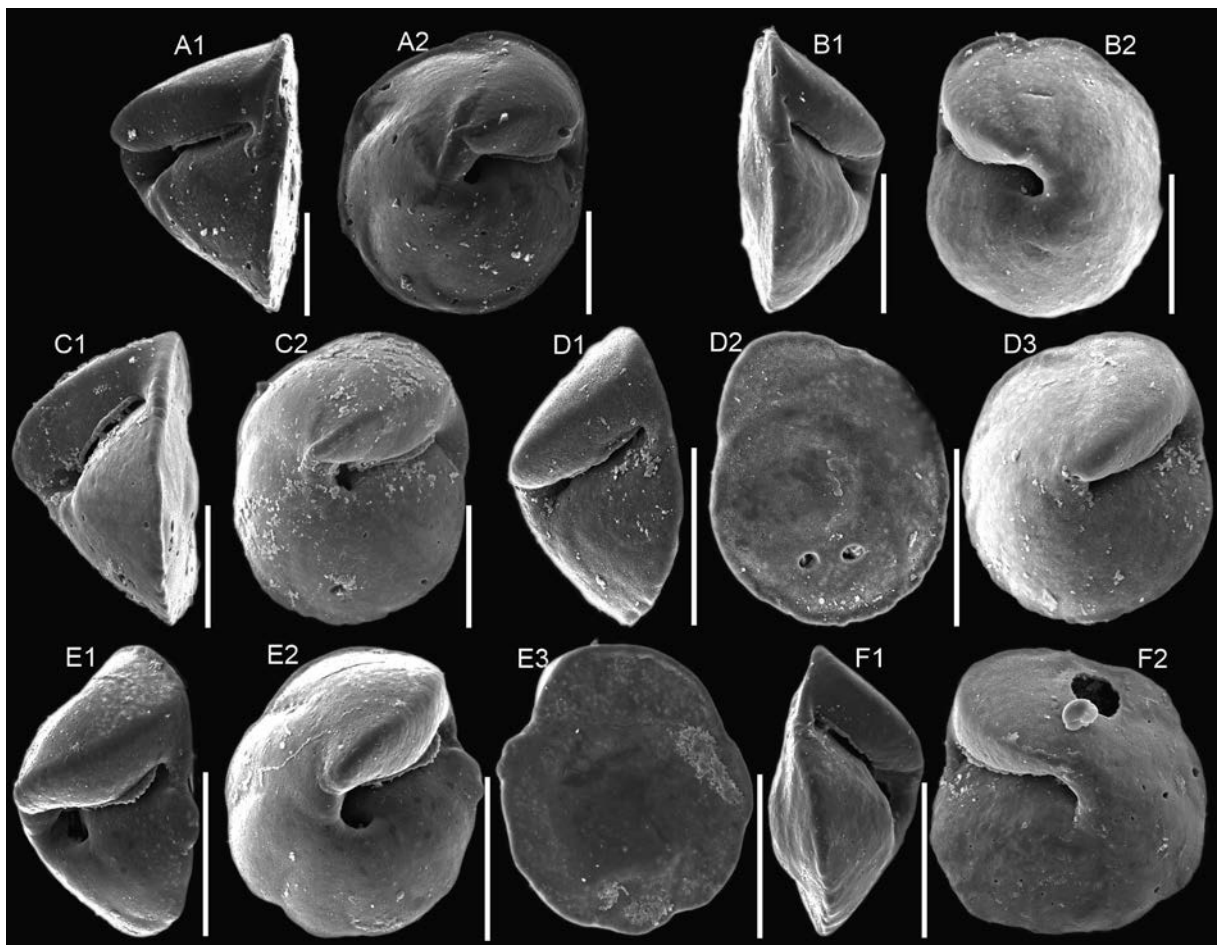
For $\delta^{13}C$ and $\delta^{18}O$ isotopic analyses, 30 monospecific foraminiferal test samples, 15 containing the

planktonic foraminifera *Globigerinelloides prairiehil-lensis* Pessagno, 1967 (50 specimens per sample) and 15 containing the benthic foraminifera *Gyroidinoides globosus* (Hagenow, 1842) (10 specimens per sample), were prepared. Isotope analyses were conducted at the GeoZentrum Nordbayern, University of Erlangen-Nuremberg, Germany. Samples were reacted with 100% phosphoric acid at 70ºC in a Gasbench II connected to a ThermoFisher Delta V Plus isotope ratio mass spectrometer (IRMS). All $\delta^{18}O$ and $\delta^{13}C$ values are reported in per mil relative to VPDB. Reproducibility and accuracy were monitored by replicate analyses of laboratory standards, calibrated by assigning $\delta^{13}C$ values of +1.95‰ to NBS19 and -47.3‰ to IAEA-CO9, and $\delta^{18}O$ values of -2.20‰ to NBS19 and -23.2‰ to NBS18. Reproducibility (1σ) over the course of sample analyses was better than ±0.06‰ for $\delta^{13}C$ and ±0.07‰ for $\delta^{18}O$.
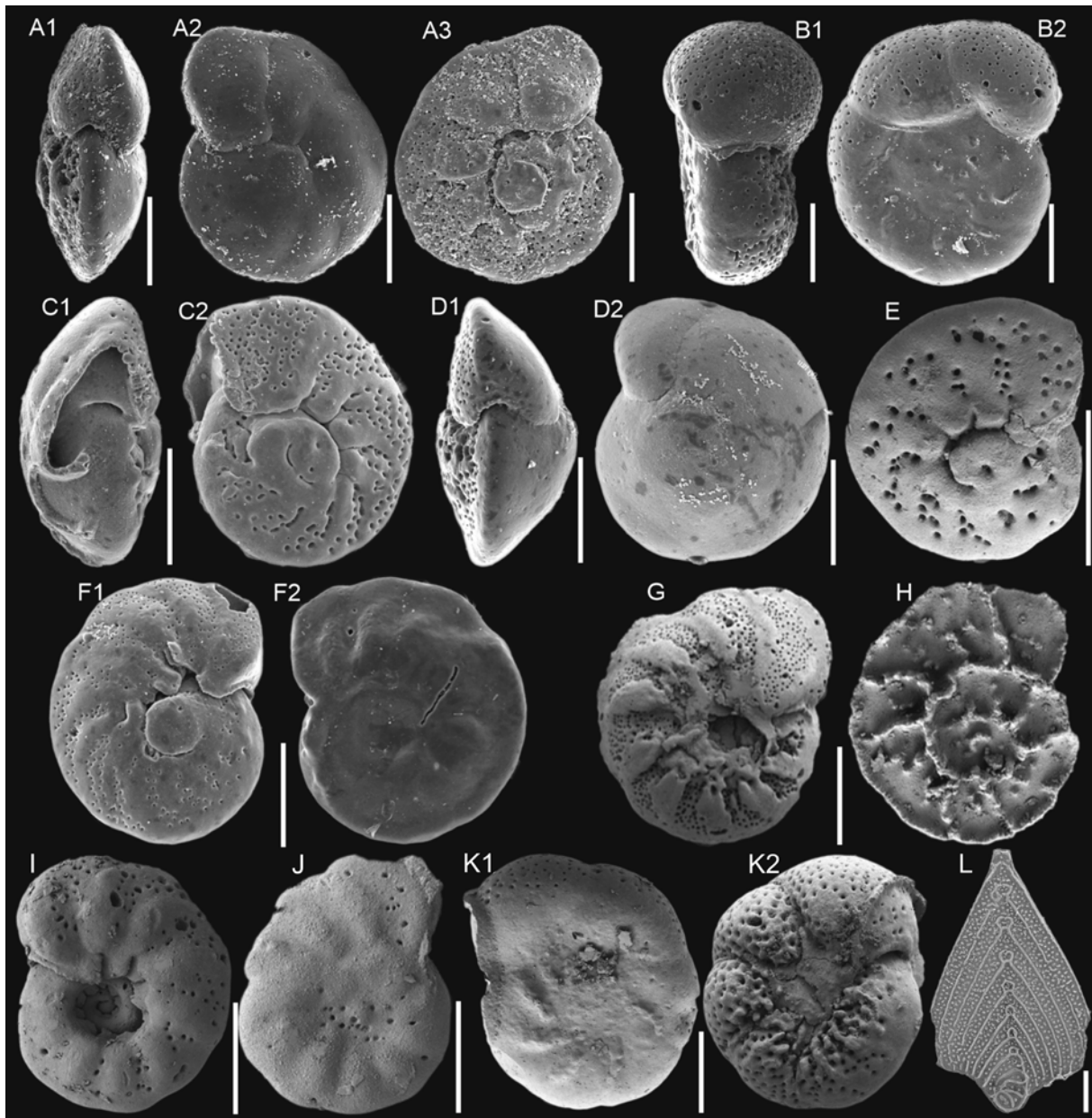
RESULTS

Foraminiferal assemblages

The investigated deposits yielded diverse, abundant, and well-preserved planktonic and benthic foraminifera (Text-figs 3–5). Foraminiferal assemblages are relatively similar throughout the studied succession, with only minor variation. Benthic foraminiferal assemblages are more taxonomically diverse than their planktonic counterparts and dominated by 6 calcareous genera: *Cibicidoides* Thalmann, 1939, *Gavelinella* Brotzen, 1942, *Globorotalites* Brotzen, 1942, *Gyroidinoides* Brotzen, 1942, *Osangularia* Brotzen, 1940, and *Stensioeina* Brotzen, 1936 (Text-fig. 6), of which only *Osangularia* is not a thick-walled morphotype. Calcareous forms account for 70.59% (sample 5) to 87.32% (sample 4) of the benthic for-
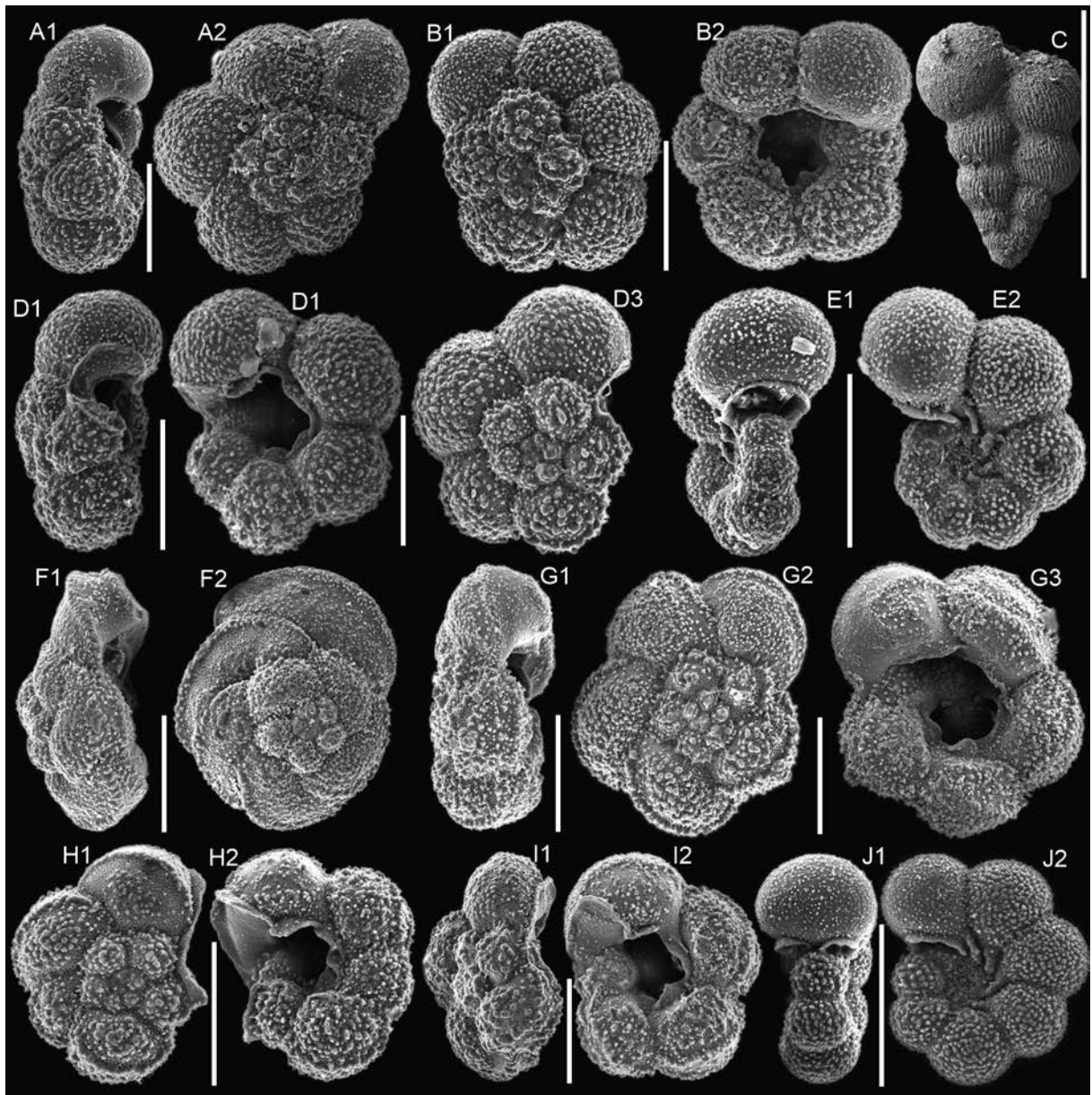

Text-fig. 3. SEM images of the foraminifera *Globorotalites* Brotzen, 1942 lineages from the Belgorod section. **A**, **C** – *G. michelinianus* (d'Orbigny, 1840), A – MWGUW ZI/67/82.10, sample 2, C – MWGUW ZI/67/82.05, sample 2. **B**, **E** – *Globorotalites* sp. 1 (transitional form between *G. michelinianus* and *G. emdyensis*), B – MWGUW ZI/67/82.03, sample 14; E – MWGUW ZI/67/82.09, sample 14. **D**, **F** – *G. emdyensis* Vasilenko, 1961, D – MWGUW ZI/67/82.07, sample 14; F – MWGUW ZI/67/82.02, sample 14.

Text-fig. 4. SEM images of selected benthic foraminifera from the Belgorod section. **A**, **F** – *Gavelinella monterelensis* (Marie, 1941), A – MWGUW ZI/67/82.12, sample 5; F – MWGUW ZI/67/82.29, sample 7. **B** – *Gavelinella annae* (Pożaryska, 1954), MWGUW ZI/67/82.13, sample 5. **C–E** – *Cibicidoides voltzianus* (d'Orbigny, 1840), C – MWGUW ZI/67/82.30, sample 7; D – MWGUW ZI/67/82.32, sample 7; E – MWGUW ZI/67/MF1-017, sample 13. **G**, **H** – *Stensioeina pommerana* Brotzen, 1936, G – MWGUW ZI/67/MF1-011, sample 6; H – MWGUW ZI/67/MF1-012, sample 2. **I**, **J** – *Gavelinella pertusa* (Marsson, 1878), I – MWGUW ZI/67/MF1-022, sample 11; J – MWGUW ZI/67/MF1-023, sample 8. **K** – *Gavelinella* ex. gr. *clementiana* (d'Orbigny, 1840), MWGUW ZI/67/MF1-024, sample 5. **L** – *Neoflabellina rugosa* (d'Orbigny, 1840), MWGUW ZI/67/82.01, sample 14.

aminifers. Large epifaunal morphotypes, including *Gavelinella*, *Globorotalites*, and *Stensioeina*, represent approximately 23% of the benthic foraminiferal assemblages. In general, there is no dominant benthic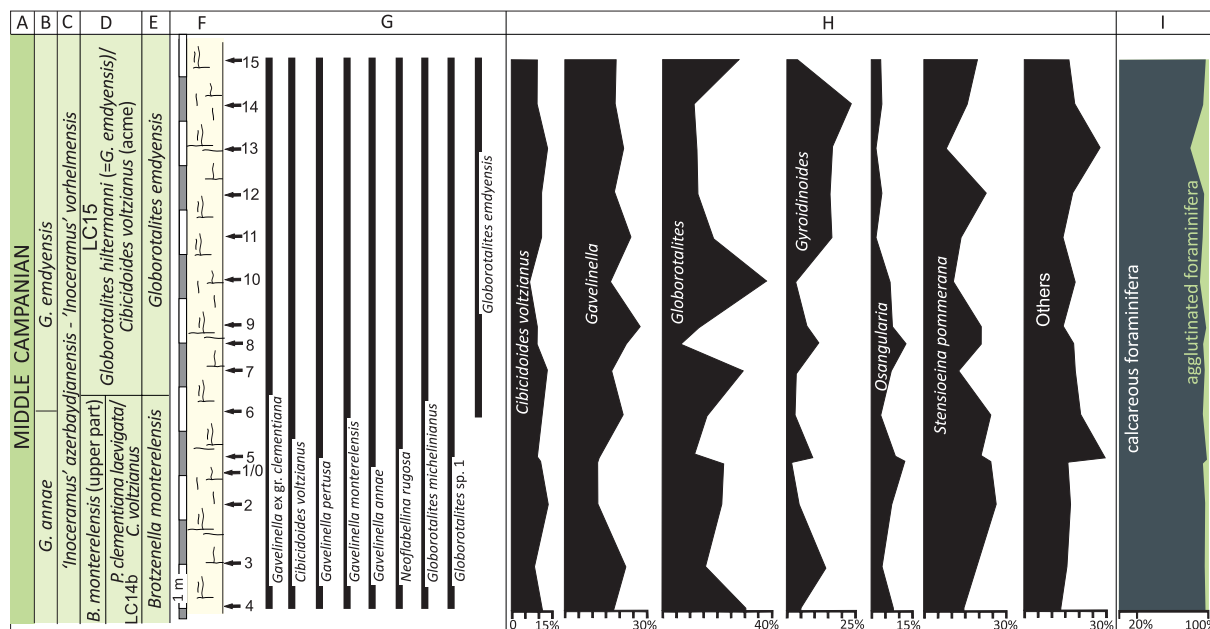 foraminiferal genus except *Globorotalites*, which ac-counts for 37.87% of specimens in sample 10. All assemblages contain Lagenida Delage and Hérouard, 1896, although its representatives do not exceed an average of 3% of benthic forms. Infaunal genera are represented by both agglutinated (*Ataxophragmium*

Text-fig. 5. SEM images of selected planktonic foraminifera from the Belgorod section. **A**, **B** – *Archaeoglobigerina bosquensis* Pessagno, 1967, A – MWGUW ZI/67/82.15, sample 5, B – MWGUW ZI/67/82.16, sample 5. **C** – *Planoheterohelix globulosa* (Ehrenberg, 1840), MWGUW ZI/67/MF1-017, sample 9. **D** – *Archaeoglobigerina blowi* Pessagno, 1967, MWGUW ZI/67/82.17, sample 5. **E** – *Globigerinelloides prairiehillensis* Pessagno, 1967, MWGUW ZI/67/82.19, sample 3. **F** – *Contusotruncana fornicata* (Plummer, 1931), MWGUW ZI/67/82.04, sample 14. **G**, **I** – *Globotruncana bulloides* Vogler, 1841, G – MWGUW ZI/67/82.08, sample 2, I – MWGUW ZI/67/82.25, sample 12. **H**– *Globotruncana hilli* Pessagno, 1967, MWGUW ZI/67/82.28, sample 12. **J** – *Globigerinelloides multispinus* (Lalicker, 1948), MWGUW ZI/67/82.26, sample 5.

Reuss, 1860, *Plectina* Marsson, 1878) and calcareous (*Praebulimina* Hofker, 1953) taxa, and constitute, on average, 5.37% of all benthic foraminifera. They are, however, somewhat more abundant in samples 5 (12.35%) and 14 (10.09%). The infauna is dominated by *Praebulimina* (average 64.35% of all

benthic taxa). 93.75% of the examined foraminifera are calcareous. Increased agglutinated abundance is noted only in samples 10 (10.04%) and 13 (19.35%). The agglutinated forms are poorly diversified and represent the following genera: *Ataxophragnium*, *Plectina*, *Spiroplectammina* Cushman, 1927b, *Tro-*

Text-fig. 6. Changes in benthic foraminiferal assemblages of the Belgorod chalk succession. The columns refer to: (A) chronostratigraphy; (B) benthic foraminiferal zonation after Dubicka (2015); (C) inoceramid zonation after Walaszczyk *et al.* (1997, 2016); (D) benthic foraminiferal zonation after Beniamovski (2007, 2008); (E) benthic foraminiferal zonation after Olfer'ev and Alekseev (2003) and Olfer'ev *et al.* (2004); (F) lithological column with sample locations; (G) vertical ranges of stratigraphically important benthic foraminifera; (H) relative abundances of dominant and common genera and species within benthic foraminiferal assemblages; and (I) calcareous-to-agglutinated benthic foraminifera ratio.
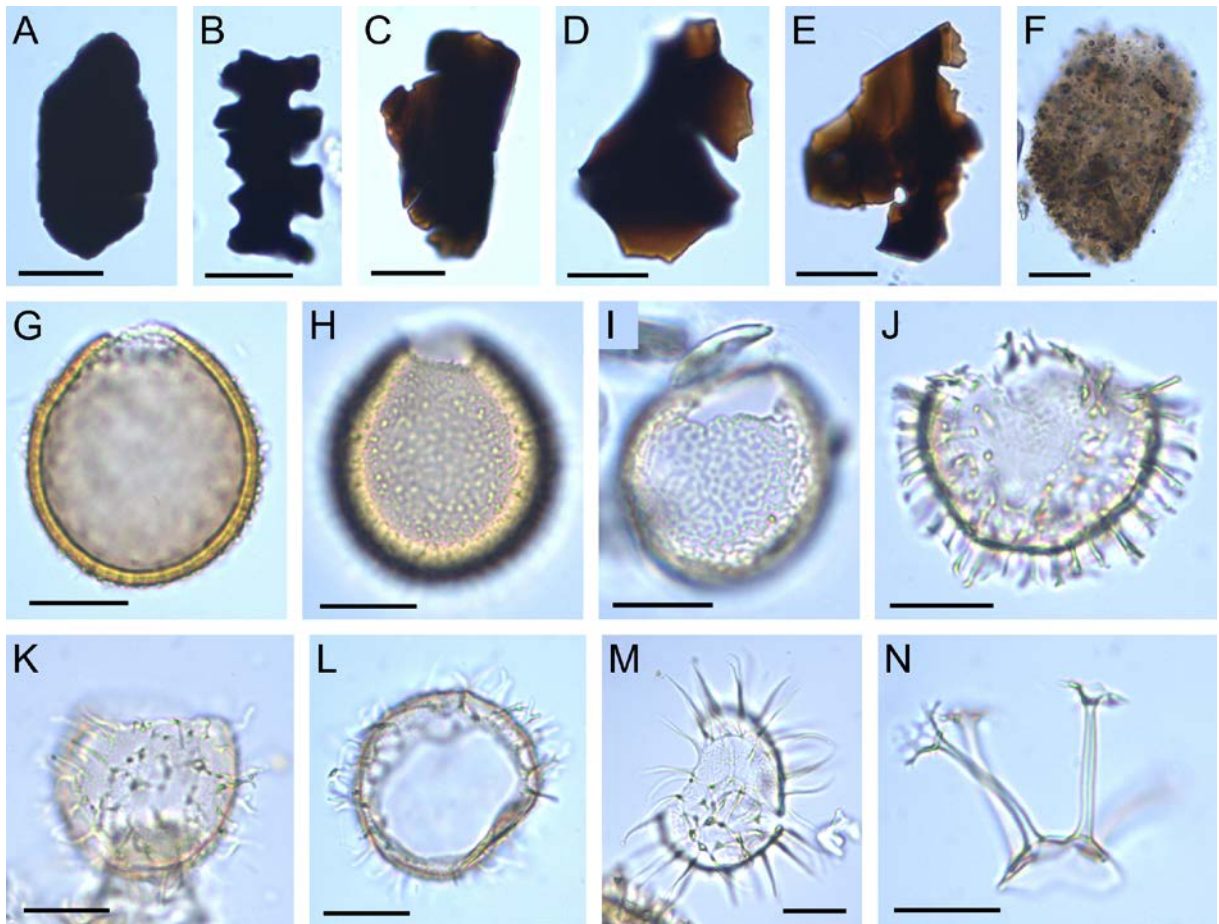
chammina Parker and Jones, 1859, emended Brönniman and Whittaker, 1983, and *Arenobulimina* Cushman, 1927a. The genus *Arenobulimina* is dominant, composing on average 63% of agglutinated assemblages, and is the only genus consistently observed in all studied samples. The percentage of planktonic foraminifera in the foraminiferal assemblages ranges from 5.62% (sample 10) to 31.73% (sample 5).

Planktonic foraminiferal assemblages are composed of 4 major morphogroups (Text-fig. 2): biserial (Heterohelicidae Cushman, 1927b), planispiral (Globigerinelloididae Longoria, 1974), trochospiral (Rugoglobigerinidae Subbotina, 1959), and keeled (Globotruncanidae Brotzen, 1942). The biserial heterohelicids almost entirely consist of the species *Planoheterohelix globulosa* (Ehrenberg, 1840) and occur in all samples. Because of their small size, they are abundant in the <100 µm fraction; as such, the relative proportion of biserial foraminifera within planktonic foraminiferal assemblages was not considered. The planispiral morphogroup is composed of *Globigerinelloides prairiehillensis* and *G. multispinus* (Lalicker, 1948), which on average compose 47.62% of planktonic assemblages. They are least abundant in sample 10 (14.29%) and most abundant

in sample 15 (80.33%). The trochospiral morphogroup (*Archaeoglobigerina bosquensis* Pessagno, 1967; *A. blowi* Pessagno, 1967) constitutes an average of 36.25% of the observed planktonic assemblages, varying from 11.27% (sample 12) to 58.82% (sample 2). The keeled morphogroup, composed of *Contusotruncana fornicata* (Plummer, 1931), *Globotruncana bulloides* Vogler, 1941, and *Globotruncana hilli* Pessagno, 1967, on average composes 16.13% of planktonic assemblages. It is absent in sample 5 and most abundant in sample 10 (57.14%).

Sedimentary organic matter

All analyzed samples yielded very low sedimentary organic matter concentrations – indeed, some samples are virtually barren. Given the scarcity of organic matter in the studied material, it was not deemed possible to perform a reliable palynofacies analysis. For the same reason, biostratigraphic and paleoenvironmental analyses based on palynomorph composition could not be performed, as both require at least 300 kerogen/palynomorph particles per sample. Nevertheless, the relative abundance of particular sedimentary organic matter constituents varies significantly throughout the
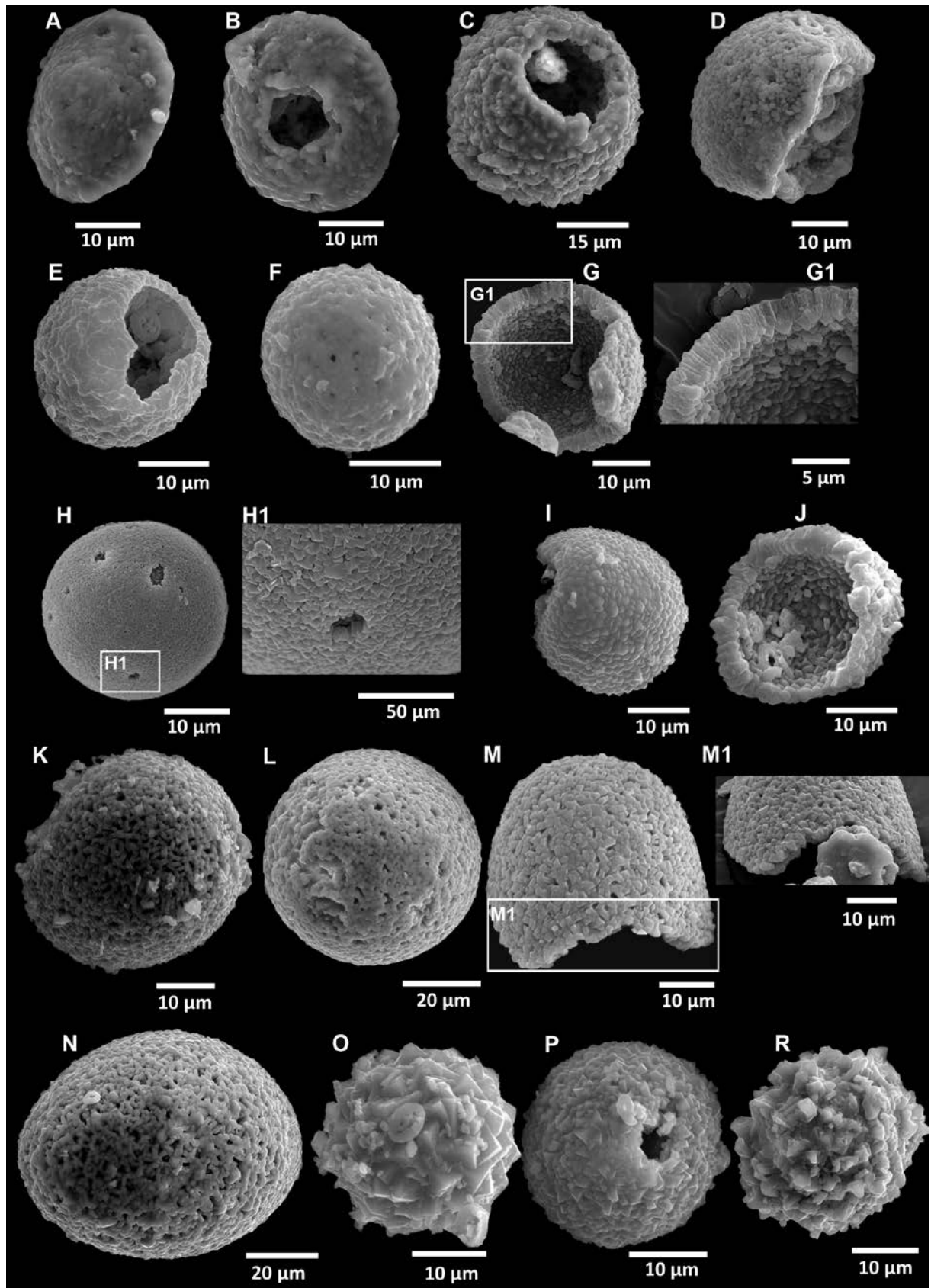
Text-fig. 7. Photomicrographs of phytoclasts (A–E), AOM (F), and organic-walled dinoflagellate cysts (G–N) from the Belgorod section. **A, B** – Opaque phytoclasts, sample 7. **C, D** – Translucent phytoclasts, sample 7. **E** – Translucent phytoclast, sample 8. **F** – AOM, sample 10. **G, H** – *Batiacasphaera solida* Slimani, 2003, sample 6. **I** – *Kallosphaeridium* sp., sample 12. **J** – *Circulodinium distinctum* (Deflandre and Cookson, 1955) Jansonius, 1986, sample 7. **K, L** – *Heterosphaeridium heteracanthum* (Deflandre and Cookson, 1955) Eisenack and Kjellström, 1972, sample 8. **M** – *Pervosphaeridium* cf. *intervelum* Kirsch, 1991, sample 9. **N** – *Oligosphaeridium complex* (White, 1842) Davey and Williams, 1966, sample 7. All photomicrographs taken using a transmitted-light microscope. Scale bars equal 20 μm.

succession, and the analysis of their distribution can provide useful paleoenvironmental data.

Translucent and opaque phytoclasts are the most frequent kerogen particles in the studied material (see Text-fig. 2). While they present in all analyzed samples, they are most common in samples 1, 6–8, and 12 (sample 7 yielded the highest phytoclast concentration). The palynomorphs are pale yellow and very rare; they are represented exclusively by organic-walled marine phytoplankton (dinocysts), have only been found in samples 1, 6–10, and 12, with the highest abundance in sample 7 (Text-fig. 2), and are of low taxonomic diversity. The dinocysts are mostly fragmented (only a few complete specimens were found), rendering it difficult to identify cysts at species or genus level. Nevertheless, the organic-walled dinocysts are predominantly of gonyaulacoid affinity (autotrophic forms), while peridinioid dinoflagellate cysts are apparently absent. *Batiacasphaera solida* Slimani, 2003, *Circulodinium distinctum* (Deflandre and Cookson, 1955) Jansonius, 1986, *Heterosphaeridium heteracanthum* (Deflandre and Cookson, 1955) Eisenack and Kjellström, 1972, *Kallosphaeridium* sp., *Oligosphaeridium complex* (White, 1842) Davey and Williams, 1966, and *Pervosphaeridium* cf. *intervelum* Kirsch, 1991 were identified (Text-fig. 7); all are long-ranging species and biostratigraphically not significant in the studied interval. AOM is almost completely absent from the present material; no cuticular particles, sporomorphs, marine or freshwater algae, or foraminiferal organic linings were found.

www.czasopisma.pan.pl

PAN
POLSKA AKADEMIA NAUK

www.journals.pan.pl

670

MICHAŁ FĄFARA *ET AL.*

			Sample number		Identifier	$\delta^{13}C$ ‰ V-PDB	$\delta^{18}O$ ‰ V-PDB		Identifier	$\delta^{13}C$ ‰ V-PDB	$\delta^{18}O$ ‰ V-PDB
			15		B15 G15	1.23	-0.25		P30 T30	1.20	-1.99
	Globorotalites emdyensis		14		B14 G14	1.71	-0.20		P29 T29	2.01	-1.17
			13		B13 G13	1.84	-0.08		P28 T28	2.31	-1.14
			12		B12 G12	1.51	0.05		P27 T27	1.91	-1.55
MIDDLE CAMPANIAN		'*Inoceramus*' *azerbaydjanensis*–'*I.*' *vorhelmensis*	11	*Gyroidinoides globosus* (benthic)	B11 G11	1.69	-0.06	*Globigerinelloides prairiehilensis* (planktonic)	P26 T26	1.88	-1.46
			10		B10 G10	1.50	0.11		P25 T25	2.25	-1.16
			9		B9 G9	1.85	0.20		P24 T24	2.33	-2.47
			8		B8 G8	1.58	0.14		P23 T23	1.98	-1.58
			7		B7 G7	1.38	0.02		P22 T22	1.80	-1.31
	Gavelinella annae		6		B6 G6	1.52	-0.10		P21 T21	2.28	-1.13
			5		B5 G5	1.68	-0.07		P20 T20	2.28	-1.28
			1/0		B1 G1	1.70	-0.02		P18 T18	2.33	-1.23
			2		B2 G2	1.83	0.31		P16 T16	2.23	-1.43
			3		B3 G3	1.87	0.05		P17 T17	2.63	-1.15
			4		B4 G4	1.87	0.27		P19 T19	2.10	-1.46

Table 2. $\delta^{13}C$ and $\delta^{18}O$ data for foraminiferal tests from the Belgorod section.

Calcareous dinoflagellate cysts

C-dinocysts were yielded in all studied samples (Table 1 and Text-fig. 8). However, the assemblages are generally of low abundance and poorly diversified. Eleven species, belonging to four genera, were recognized (Text-fig. 8): *Fuettererella deflandrei* (Kamptner, 1956) Hildebrand-Habel and Streng, 2003; *Lentodinella danica* Kienel, 1994; *Orthopithonella* aff. *gustafsonii* (Bolli, 1974) Lentin and Williams, 1985; *Orthopithonella porata* (Keupp, 1982) Lentin and Williams, 1985; *Orthopithonella* sp. A (Keupp and Mutterlose, 1984) Streng, Hildebrand-Habel and Willems, 2002; *Orthopithonella* sp. B; *Orthopithonella* sp. C; *Pirumella edgarii* (Bolli, 1974) Lentin and Williams, 1993; *Pirumella cylindrica* (Pflaumann and Krasheninnikov, 1978) Lentin and Williams, 1993; *Pirumella loeblichii* (Bolli, 1974) Lentin and Williams, 1993; and *Pirumella thayeri* (Bolli, 1974) Lentin and Williams, 1993.
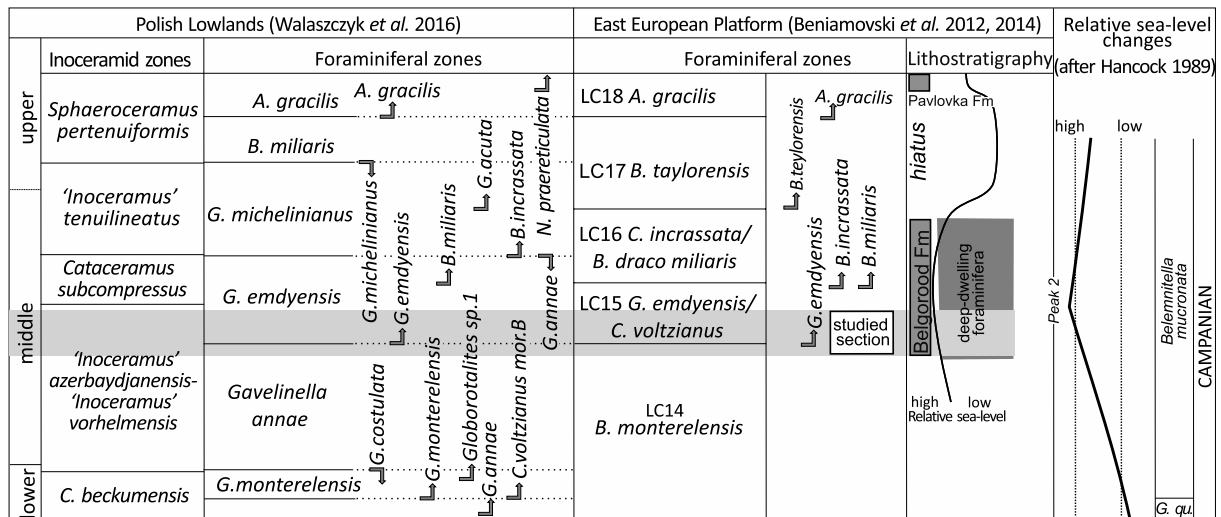
The recorded forms represent four different wall ultrastructures: oblique, pithonelloid, radial, and tangential. The radial wall is represented by *Orthopithonella* spp., the oblique wall by *Pirumella* spp. (Bolli, 1980) Streng, Basanova, Rehakova and Willems, 2009, the pithonelloid wall by *L. danica*, and the tangential wall by *F. deflandrei.* A slightly higher species diversity of radial forms than oblique forms is observed in samples 3, 9, and 11. Their species diversity is equal in sample 5, while in sample 15 the species diversity of oblique forms is slightly higher than the radial forms. While specimen abundance is relatively low in the studied samples, the richest c-dinocyst community is in sample 15; less rich communities occur in samples 3 and 5, and c-dinocysts are rare in samples 9 and 11 (Table 1). The highest species diversity is noted in sample 15 (9 specimens), while the lowest diversity is noted in samples 11 and 9 (5 and 6 species, respectively). Most recognized species are long ranging. However, *Pirumella cylindrica* is biostratigraphically important, as it ranges from the Campanian to the Maastrichtian (Pflaumann and Krasheninnikov 1978). *Lentodinella danica* is also potentially of biostratigraphic importance, with its first occurrence in the Campanian (Streng *et al.* 2004) and a last occurrence in the Danian of the early Paleocene (Wendler and Willems 2002).

Foraminiferal test $\delta^{13}C$ and $\delta^{18}O$ values

$\delta^{13}C$ and $\delta^{18}O$ analyses were performed on monospecific *Gyroidinoides globosus* (benthic) and

← Text-fig. 8. SEM photomicrographs of c-dinocysts from the Belgorod section. **A, B** – *Lentodinella danica* Kienel, 1994, sample 15. **C, D** – *Fuettererella deflandrei* (Kamptner, 1956) Hildebrand-Habel and Streng, 2003, sample 15. **E** – *Orthopithonella* aff. *gustafsonii* (Bolli, 1974) Lentin and Williams, 1985, sample 5. **F** – *Orthopithonella porata* (Keupp, 1982) Lentin and Williams, 1985, sample 3. **G** – *Orthopithonella* sp. A, sample 15; G1 – magnified view of test wall, showing internal texture. **H** – *Orthopithonella* sp. B, sample 15; H1 – magnified view of test surface, showing calcite crystals. **I, J** – *Orthopithonella* sp. C, samples 9 (I) and 5 (J). **K, L** – *Pirumella edgarii* (Bolli, 1974) Lentin and Williams, 1993, samples 3 (K) and 15 (L); **M, N** – *Pirumella cylindrica* (Pflaumann and Krasheninnikov, 1978) Lentin and Williams, 1993, samples 5 (M) and 15 (N); M1 – magnified view of cysts showing internal texture of the wall. **O, P** – *Pirumella loeblichii* (Bolli, 1974) Lentin and Williams, 1993, samples 3 (O) and 15 (P); **R** – *Pirumella thayeri* (Bolli, 1974) Lentin and Williams, 1993, sample 15.

Text-fig. 9. Stratigraphic position of the Belgorod chalk (dark grey area) and correlation of the Belgorod Formation with the Campanian transgressive peak no. 2. *G. qu. – Gonioteuthis quadrata*.

Globigerinelloides prairiehillensis (planktonic) samples. The studied foraminiferal tests were devoid of sediment infilling and were excellently preserved. The pores were open, with no internal sediment or mineral phase crystallization. The test textures displayed original nanotextures (see Dubicka 2019) with no evidence of dissolution or recrystallization. $\delta^{13}C$ values are consistently higher for the planktonic taxon than for the benthic taxon (Text-fig. 2; Table 2), while $\delta^{18}O$ values are consistently higher in the benthic foraminifera. $\delta^{18}O$ values vary between -2.47‰ (sample 9) to -1.13‰ (sample 6) for *Gl. prairiehillensis* (average -1.43‰) and from -0.25‰ (sample 15) to 0.31‰ (sample 2) for *G. globosus* (average 0.02‰). $\delta^{13}C$ values rise from 1.20‰ (sample 15) to 2.63‰ (sample 3) for *Gl. prairiehillensis* (average 2.1‰) and from 1.23‰ (sample 15) to 1.87‰ (sample 4 and 3) for *G. globosus* (average 1.65‰). $\delta^{13}C$ values of both taxa fluctuate with a ~0.6‰ amplitude throughout the entire profile, with the lowest $\delta^{13}C$ values in samples 7 and 15. The planktonic $\delta^{18}O$ curve fluctuates more than the corresponding benthic curve, which is comparatively stable. Intriguingly, the planktonic $\delta^{18}O$ curve generally corresponds with increasing/decreasing trends in the $\delta^{13}C$ curves.

DISCUSSION

Biostratigraphy

The studied samples yielded stratigraphically important benthic foraminifera: *Gavelinella annae* (Pożaryska, 1954), *Gavelinella monterelensis* (Marie, 1941), *Globorotalites michelinianus* (d'Orbigny, 1840), *Globorotalites emdyensis* Vasilenko, 1961, *Gavelinella* ex. gr. *clementiana* (d'Orbigny, 1840) and *Neoflabellina rugosa* (d'Orbigny, 1840) (Text-fig. 4; see Text-fig. 9 for ranges of the first four taxa). These taxa are indicative of the upper LC14b and lower LC15 zones proposed for the Russian Platform (Beniamovskiy *et al.* 2012, 2014) and the upper *Gavelinella annae* Zone and lower *Globorotalites emdyensis* Zone in the Polish Lowlands foraminiferal zonation (Dubicka 2015; Walaszczyk *et al.* 2016). The zonal boundaries lie in the middle of the studied succession (between samples 6 and 7), at the first occurrence of *G. emdyensis* (Text-fig. 6). The foraminiferal-based stratigraphic position of the studied section correlates with the upper '*Inoceramus*' *azerbaydjanensis*–'*Inoceramus*' *vorhelmensis* inoceramid Zone (Walaszczyk 1997), corresponding to the Middle Campanian in the American tripartite stage subdivision (see Walaszczyk *et al.* 2008).

The very unusual deep-water planktonic foraminiferal community, the paucity of terrigenous material (Beniamovskiy *et al.* 2014) and the higher species diversity of obliquipithonelloids (oblique wall c-dinocyst group) compared to orthopithonelloids (radial wall c-dinocyst group) (Keupp 1993; Kohring 1993) suggest that the Belgorod chalk was deposited during a sea-level highstand. This eustatic high observed in the Belgorod section corresponds to transgressive peak no. 2 of Hancock (1989, 1993). In north-western Europe, this peak is placed in the Middle Campanian *Belemnitella mucronata* Zone (Reid 1973; Hancock 1989), and the same age is recognized in Lower Saxony,

north-central Germany (Niebuhr *et al.* 1997; Niebuhr 1999; Niebuhr and Reich 2004). In Poland, peak no. 2 is observed in the lower *Neancyloceras phaleratum* Zone of Błaszkiewicz (1980) in the Middle Vistula River section (Christensen 1990; Hancock 1993) near Sulejów, corresponding to the *Globorotalites emdyensis* foraminiferal Zone (Walaszczyk *et al.* 2016). In North America, the Middle Campanian peak correlates with: (i) the middle of the Claggett Shale, (ii) the uppermost *Baculites mclearni* Zone of Montana, and (iii) the Pecan Gap Chalk of Texas (Hancock 1993).

Water depth versus distance from the shoreline: impacts on chalk deposition

The Belgorod chalk is a very unique lithofacies compared to other regional Cretaceous deposits: it contains the highest amount of calcium carbonate (c. 95%) and the lowest amount of terrigenous material of the entire Middle Campanian to upper Maastrichtian succession in central European Russia (Beniamovskiy 2014).

Chalk is the most characteristic Cretaceous lithofacies, with vast distributions in both hemispheres (Skelton 2003). It was the most abundant limestone lithofacies in mid-latitudinal epicontinental seas during the Late Cretaceous eustatic highstand. Chalk largely consists of tiny calcitic coccolithophore skeletons, with an admixture of other calcite bioelements (e.g., foraminiferal tests, inoceramid prisms, calcispheres) that accumulated as ooze. Since the Eocene, calcareous ooze almost exclusively forms in oceanic deposits, so the massive accumulation of chalk over vast areas of inundated continental seas is rather non-uniformitarian. The depositional setting(s) of chalk facies, especially with regard to paleobathymetry, are still contested (see, e.g., Puckett 1991). In the Cretaceous, chalk could have been deposited along a variety of depths, ranging from shallow-water to relatively deep-water settings. The maximum depth for calcareous ooze accumulation is limited by the carbonate compensation depth, which latitudinally varies from ~4,000 m in the tropics to several hundred meters in the Southern Ocean. The minimum water depth of Cretaceous chalk is limited by the position of the storm wave base, estimated for moderate to high storm settings to approximately 90 m (Lasseur *et al.* 2009). Different premises lead to even shallower minimum chalk paleobathymetry, for instance 65–90 m (Puckett 1991) or 50 m depth (Kennedy 1970). In general, however, the average bathymetric position of chalk is mostly estimated to lie between approximately 80 and 600 m depth (Reid

1968; Hancock 1975). However, as chalk is a purely calcareous sediment deposited with minimal terrigenous influx, distance from the shoreline is also an important factor controlling the distribution of chalk sedimentation. In general, chalk occupies a more distal, deeper water position than opoka (spiculitic limestone) or gaize (carbonate with higher detrital quartz content) when these facies are present in a single facies tract (Walaszczyk and Remin 2015; Machalski and Malchyk 2019). That is, the main factors influencing lithofacies distribution in Cretaceous basins were distance from the shoreline and topography (Leszczyński 2010, 2012). Therefore, chalk was a characteristic epicontinental facies during sea-level highstands, when emergent land areas were reduced (Wiese *et al.* 2015). An excellent example is provided by the Maastrichtian of the Middle Vistula River section (see Pożaryski 1948 for detailed description and stratigraphy), which captures a maximum in sea-level (Dubicka and Peryt 2012) corresponding to global Peak 4 of Hancock (1993) and the "*junior* Transgression" of Niebuhr (1995). In the Vistula section, this event coincides with the disappearance of opoka – the dominant facies in the upper Campanian–Maastrichtian succession – and the development of chalk facies with no detrital quartz, glauconite, or sponge spicules. Likewise, during the late Cenomanian and Turonian, pelagic calcareous nannofossil ooze was widely distributed on the European shelf during the peak Cretaceous transgression (Wiese *et al.* 2015).

That being acknowledged, chalk can also constitute a relatively shallow facies, as documented by the upper Turonian chalk in Dubivtsi Quarry south of Halych (Western Ukraine), deposited under <100 m depth. Intriguingly, this comparatively shallow chalk is a very pure calcareous facies (97.8% to 99.9% $CaCO_3$), with almost no detrital contribution (Dubicka *et al.* 2014). The genesis of this phenomenon becomes clear in the context of the Cretaceous paleogeography and tectonic evolution of western Ukraine. During the Turonian, western Ukraine and eastern Poland were covered by a wide epicontinental sea that freely connected with the Tethys to the south. The nearest coastline, associated with the emergent Ukrainian Shield, was at least 300 km away (Pasternak *et al.* 1968; Scotese 2014). Importantly, this is a comparable distance to that between the Lower Saxony Basin and the nearest land masses during the Turonian, during which the Salder Formation was composed of up to 90% $CaCO_3$ (Wiese *et al.* 2015). Beginning in the latest Turonian, western Ukraine was impacted by Subhercynian tectonic movements related to compressional stress transmit-

ted into the foreland from the Alpines (Vejbæk and Andersen 2002). Consequently, the area southwest of the Dubivtsi section was uplifted and transformed into the "Kukernitz Island" of Pasternak (1959), which subsequently supplied terrigenous material to the studied basin (Pasternak *et al.* 1968, 1987).

Similarly, the Belgorod chalk is characterized by a very high $CaCO_3$ content (c. 95%), with only minor non-carbonate contributions (Beniamovskiy 2014). In conjunction with previous work on mineralogical composition, our observations of (i) very low terrestrially-sourced plant debris concentrations (translucent and opaque phytoclasts), (ii) the lack of cuticular material, and (iii) the absence of sporomorphs indicate that the basin was quite distal from any emergent land. It is consistent with the onset of a sea-level highstand, as supported by (i) diverse, deep-dwelling planktonic foraminiferal communities with relatively high ratios of keeled forms, such as *Globotruncana* Cushman, 1927b and *Contusotruncana* Korchagin, 1982, and (ii) higher species diversity of obliquipithonelloids compared to orthopithonelloids (see Keupp 1993; Kohring 1993). This planktonic foraminiferal community suggests that water depth during deposition was greater than 100 m (see Hart and Bailey 1979; Caron and Homewood 1983; Leckie 1987; Rebotim *et al.* 2017). In this context, it is worth observing that Savko and Ivanova (2009) interpreted the paleodepth of the Belgorod chalk as approximately 400 m. Nevertheless, despite the absence of robust, absolute paleobathymetry, a significant sea-level rise seems to be plausible and supported by both lithological and paleontological records. It temporally corresponds with peak no. 2 of Hancock (1993), a Middle Campanian sea-level highstand recognized in central and north-western Europe (Hancock 1989; Niebuhr *et al.* 1997; Niebuhr 1999, 2006; Kaplan 2004; Niebuhr and Reich 2004), the US Western Interior (Hancock 1993), and possibly New Zealand (Schiøler *et al.* 2002).

An oligotrophic continental shelf setting

The low concentration of terrestrially-sourced plant debris (translucent and opaque phytoclasts) in the present material, and the complete absence of cuticular material and sporomorphs, indicate that the studied succession was deposited at a considerable distance from the shore. Given that rich dinocyst assemblages are commonly reported in chalk facies (e.g., Schiøler and Wilson 1993; Slimani 2001; Surlyk *et al.* 2013), the scarcity of organic-walled marine phytoplankton in the present material may

appear surprising, especially as they are exclusively represented by rare gonyaulacoid (autotrophic) dinocysts. It should be noted that dinoflagellates flourish in relatively shallow marine settings; their highest diversities are reached along continental margins and decrease significantly offshore (e.g., Pross and Brinkhuis 2005; de Vernal *et al.* 2020). Therefore, their poor representation in an open marine basin, in particular a distal offshore environment, is understandable. Indeed, a comparable relationship between deeper water, more offshore conditions (related to second-order maximum flooding) and low palynomorph abundance and dinocyst diversity is well documented in the Campanian chalk of the Paris Basin (Pearce *et al.* 2022).

Peridinioid dinocysts were not observed in the present material. In contrast to autotrophic dinocysts, many peridinioids are heterotrophs (e.g., Harland 1988), and most commonly occur in nutrient-rich settings, such as estuarine systems and upwelling zones (e.g., Wall *et al.* 1977; Powell *et al.* 1992; Prauss 2000); they are rare and/or completely absent in oligotrophic environments (e.g., Olde *et al.* 2016). Likewise, foraminiferal organic linings and prasinophyte algae tend to be more abundant in high-productivity areas (e.g., Powell *et al.* 1996; Prauss 2000; Hardy and Wrenn 2009). Hence, the absence of peridinioid dinocysts, prasinophyte algae, and foraminiferal organic linings in this section is consistent with a eustatic highstand interpretation. Very low AOM concentrations are also consistent with a highstand, since AOM is generated by microbes via the degradation of marine phytoplankton, fecal pellets, and organic aggregates (e.g., Tyson 1995). In principle, poor dinocyst recovery can be driven by extremely high bottom water oxygen levels and/or thermal maturation. The latter can certainly be excluded, since all of the palynomorphs are pale yellow, suggesting little to no thermal maturation (e.g., Tyson 1993). Bottom water oxygenation may, however, be an important factor controlling the local palynological record (e.g., Pross 2001; Zonneveld *et al.* 1997). Prolonged exposure of deposited organic matter to oxygen may cause intra- and/or post-depositional oxidation, resulting in the aerobic degradation of palynomorphs (e.g., Zonneveld *et al.* 1997, 2008; Radmacher and Uchman 2020; Radmacher *et al.* 2021). While the benthic foraminifera recovered from the present material are indicative of a highly oxygenated environment, aerobic degradation of palynomorphs was most likely not an important consideration. The lack of any physical signs of reduced sedimentation rates (e.g., glauconite, hardgrounds, fossil accumulations) suggests a relatively high sedimenta-

tion rate that hindered sediment oxygen penetration, thus impeding organic matter degradation (Zonneveld *et al.* 1997). Additionally, aerobic degradation would have resulted in the oxidation of translucent woody material and its transformation into opaque phytoclasts, leading to the dominance of the latter in microscopic plant debris assemblages (e.g., Tyson 1993; Radmacher *et al.* 2021); this is not observed here. The scarcity of organic-walled dinoflagellate cysts is even more surprising, considering that the other microplankton groups (calcareous nannofossils and foraminifers) are well represented. However, when calcareous nannofossils are most abundant in pelagic carbonates, the associated organic matter content may simply be diluted by very high carbonate concentrations. Moreover, the highest relative nannofossil abundances are noted under oligotrophic oceanic conditions (Bown *et al.* 2004). In deeper, more distal settings with strongly limited nutrient availability, conditions would be unfavorable even for autotrophic dinoflagellates.

Collectively, it appears that dinoflagellates and other organic-walled phytoplankton were simply rare, or even absent, from this part of the basin. The existence of oligotrophic conditions is also supported by benthic foraminifera, which in all studied samples are dominated by calcareous epifaunal forms with large, thick-walled, and low-trochospiral tests, i.e., *Cibicidoides voltzianus* (d'Orbigny, 1840), *Gavelinella* sp., *Globorotalites michelinianus*, *Stensioeina pommerana* Brotzen, 1936, with few agglutinated and infaunal species. According to the foraminiferal TROX model (Kaiho 1991; Jorissen *et al.* 1995; Van der Zwaan *et al.* 1999), these large, calcareous epifaunal forms are a good proxy for highly oxygenated, oligotrophic environments. The very low ratio of agglutinated and infaunal forms is also suggestive of organic-poor sediments and low biological productivity (see Dubicka *et al.* 2014).

Analogous paleoceanographic conditions have been observed through the late Cenomanian and early Turonian in the Anglo-Paris Basin (Gale *et al.* 2000; Linnert *et al.* 2010), where the onset of pure chalk facies started during a transgression that triggered oligotrophic conditions. The highly oligotrophic Turonian blue-water system on the European shelf, extending from England to Russia (the pelagic European epicontinental sea; Wiese *et al.* 2015, 2018), was associated with widespread chalk or chalk-like calcareous nannoplankton/foraminifera/c-dinocyst deposits. These facies were associated with the peak Cretaceous transgression (Wiese *et al.* 2015), before the extensive Late Cretaceous basin inversions in Central Europe (see

Voigt *et al.* 2021) during the Coniacian–Campanian that resulted in a widespread transition from hemipelagic limestones to marly sediments.

High-order sea-level fluctuations reflected in microfossil and isotopic records

Although low in all analyzed samples, sedimentary organic matter concentrations vary significantly throughout the succession. The highest abundances (predominantly dinocysts and translucent and opaque phytoclasts) are observed in samples 6–8 (Text-fig. 2); sample 7 has the richest phytoclast and palynomorph record. Collectively, this suggests that samples 6–8 capture an interval of relatively increased terrestrial organic matter input and higher organic-walled dinoflagellate cyst productivity. Consequently, it is interpreted as a shallower, more proximal interval than the remainder of the studied succession. Likewise, planktonic foraminifera assemblages are highly depleted in deep-dwelling forms in this interval. And, moreover, a higher diversity of radially-walled orthopithonelloids compared to obliquely-walled obliquipithonelloids (Keupp 1993; Kohring 1993) is observed in samples 3, 9, and 11, suggestive of deeper and/or more offshore conditions below and above the discussed interval. The equal species diversity of radial and oblique wall species in sample 5, and the higher oblique/radial species diversity ratio in sample 15, indicate shallowing of the basin during these intervals. High-order sea-level oscillations are also reflected by the planktonic and benthic foraminifera $\delta^{13}C$ and planktonic foraminifera $\delta^{18}O$ records. Such trends are, however, not depicted in $\delta^{18}O$ values for epifaunal foraminifera, which are more stable within the succession. The two negative $\delta^{13}C$ peaks associated with the eustatic lowstand intervals (samples 6–8 and 14–15) are probably related to an influx of ^{12}C-enriched continental runoff via rivers, and potentially also via groundwater and aerosols (Kwon *et al.* 2021).

The transfer of carbon from terrestrial to oceanic environments (estimated at 1.4±0.5 GtC per year; Kwon *et al.* 2021) represents an important part of the global carbon cycle and an essential link between terrestrial, atmospheric and oceanic carbon pools, and therefore has a significant imprint on oceanic $\delta^{13}C$ distribution (Chaplot and Mutema 2021). The major mechanism of terrestrial to oceanic carbon transfer is river runoff (c. 8.4 GtC per year; Chaplot and Mutema 2021), the main driver of which is soil erosion (land degradation; e.g., Paustian *et al.* 2019). The global soil organic carbon pool is a significant carbon reservoir, containing 1400–1500 GtC – that is, twice the quantity

of carbon in the atmosphere and in all plant and animal life combined (Paustian *et al.* 2019). Most riverine dissolved carbon is inorganic (92%), with organic carbon forming a much smaller share (8%). In turn, this runoff does have an impact on seawater $\delta^{13}C_{DIC}$ (Chaplot and Mutema 2021), in particular during regressive events that expose shelf areas, increase winnowing, and drive nutrient and dissolved inorganic carbon (DIC) input into basins. Any potential increase in biological productivity during sea-level lowstands (see Birch *et al.* 2013; Wendler *et al.* 2013; Dubicka *et al.* 2018) might not be strong enough to balance the negative $\delta^{13}C$ input in this oligotrophic environment. Terrestrial organic matter is markedly depleted in ^{13}C, with average $\delta^{13}C$ values between -34‰ and -10‰ (Marwick *et al.* 2015) – markedly lower than seawater $\delta^{13}C$ values, which characteristically range between -2‰ and -1‰ (Schmittner *et al.* 2017).

Interestingly, the positive and negative $\delta^{13}C$ trends correspond with planktonic foraminifera $\delta^{18}O$ trends, which capture changes in surface water $\delta^{18}O$ (that is, above the thermocline). The synchronous negative $\delta^{13}C$ and $\delta^{18}O$ shifts might be linked with a freshwater and/or meteoric water influx, shifting the $\delta^{18}O$ composition of surface waters to more negative values (Cooper *et al.* 2022). Additionally, the observed negative $\delta^{18}O$ isotopic shift in planktonic foraminifera during sea-level fall might have been strengthened by the foraminiferal DIC effect – that is, the observation that the $\delta^{18}O$ of planktonic foraminiferal tests decreases with increasing DIC concentrations (see Spero *et al.* 1997).

CONCLUSIONS

Planktonic and benthic foraminifera, organic-walled and calcareous dinocysts, sedimentary organic matter, and $\delta^{13}C$ and $\delta^{18}O$ values of benthic and planktonic foraminiferal tests have been studied in the Middle Campanian Belgorod succession (central European Russia) in the east-central North European epicontinental Basin, which records a sea-level rise interpreted as a eustatic highstand corresponding to the Campanian peak no. 2 of Hancock (1993). The studied succession represents the boundary interval of the *Gavelinella annae–Globorotalites emdyensis* foraminiferal Zones, corresponding to the '*Inoceramus*' *azerbaydjanensis*–'*Inoceramus*' *vorhelmensis* inoceramid Zone.

Open marine pelagic sedimentation resulted in the deposition of a pure chalk with insignificant terrigenous material content. The limited terrestrial nu-trient influx caused the development of oligotrophic conditions, controlling the distribution pattern of benthic foraminifera and organic-walled phytoplankton communities.

The existence of a deep and open marine environment in the Belgorod succession is well-supported by: (1) the presence of deep-water planktonic foraminifers such as *Globotruncana* and *Contusotruncana*; (2) very low terrestrially-derived plant debris (phytoclasts) concentrations; (3) the lack of cuticular material and sporomorphs; and (4) the higher species diversity of obliquipithonelloid relative to orthopithonelloid c-dinocysts. The succession is also characterized by a scarcity of organic-walled marine phytoplankton (very rare dinocysts; no acritarchs or algae). This feature is interpreted as primary, due to the significant paleodepth and considerable distal position of the study locality within the basin. An explanation of this feature through post-depositional processes (oxidation and/or thermal maturation) seems unlikely because: (1) the relatively fast sedimentation rate of the carbonate-rich Belgorod chalk apparently precluded oxygen-related alteration of sedimentary organic matter; and (2) the pale color of palynomorphs and phytoclasts excludes thermal maturation. High-order sea-level fluctuations, well-documented by the planktonic foraminifera record, are additionally reflected by varying phytoclast and dinoflagellate cyst concentrations and the $\delta^{13}C$ and $\delta^{18}O$ curves. All indices were largely driven by variations in terrestrial organic matter and freshwater influxes. Our data demonstrates that the main factor driving the sedimentary and trophic development of Cretaceous epicontinental seaways was proximity to land, as a function of water-column depth and topography.

REFERENCES

Avnaim-Katav, S., Almogi-Labin, A., Kanari, M. and Herut, B. 2020. Living benthic foraminifera of southeastern Medi-

terranean ultra-oligotrophic shelf habitats: Implications for ecological studies. *Estuarine*, *Coastal and Shelf Science*, **234**, 106633.

Baraboshkin, E.Yu., Lipnitskaya, T.A. and Guzhikov A.Yu. 2018. Cretaceous system of Russia and the near abroad: the problems of stratigraphy and paleogeography. Proceedings of Ninth All-Russian Conference (with international participation), Belgorod State National Research University, September 17–21, 2018, 312 pp. Polyterra; Belgorod.

Beniamovski, V.N. 2007. Benthic foraminifera zonation in the European Paleogeographic Province (EPP) as depicting their evolution. In: Musatov, V., Pervushov, E., Guzhikov, A. and Fomin, V. (Eds), Proceedings of the Third All-Russia Conference "Cretaceous System of Russia and Adjacent Areas: Problems of Stratigraphy and Paleogeography", 26–27. SO EAGO; Saratov. [In Russian]

Beniamovski, V.N. 2008. Infrazonal biostratigraphy of the Upper Cretaceous in the East European province based on benthic foraminifers, Part 1: Cenomanian–Coniacian. *Stratigraphy and Geological Correlation*, **16**, 257–266.

Beniamovskiy, V.N., Alekseev, A.S., Ovechkina, M.N., Vishnevskaya, V.S., Podgaetskii, A.V. and Pronin, V.G. 2012. Upper Campanian–lower Maastrichtian sections of the northwestern Rostov region. Article 1. Description, paleontological assemblages, and lithobiostratigraphy. *Stratigraphy and Geological Correlation*, **20**, 346–379.

Beniamovskiy, V.N., Alekseev, A.S., Podgaetskii, A.V., Ovechkina, M.N., Vishnevskaya, V.S., Kopaevich, L.F. and Pronin, V.G. 2014. Upper Campanian–lower Maastrichtian sections of northern Rostov oblast: Article 2. Depositional environments and paleogeography. *Stratigraphy and Geological Correlation*, **22**, 518–537.

Birch, H., Coxall, H.K., Pearson, P.N., Kroon, D. and O'Regan, M. 2013. Planktonic foraminifera stable isotopes and water column structure: Disentangling ecological signals. *Marine Micropaleontology*, **101**, 127–145.

Blakey, R.C. 2014. European Paleogeographic Maps – Late Cretaceous (75 Ma). Ron Blakey and Colorado Plateau Geosystems, INC. http://cpgeosystems.com/75_Cret_EurMap_sm.jpg (accessed 28 November 2014).

Błaszkiewicz, A. 1980. Campanian and Maastrichtian ammonites of the Middle Vistula River Valley, Poland: a stratigraphic-paleontological study. *Prace Instytutu Geologicznego*, **92**, 3–63.

Bolli, H.M. 1974. Jurassic and Cretaceous Calcisphaerulidae from DSDP Leg 27, eastern Indian Ocean. *Initial Reports of the Deep Sea Drilling Project*, **27**, 843–907.

Bolli, H.M. 1980. Calcisphaerulidae and Calpionellidae from the Upper Jurassic and Lower Cretaceous of D.S.D.P. Hole 416A, Moroccan Basin. *Initial Reports of the Deep Sea Drilling Project*, **50**, 525–543.

Bown, P.R., Lees, J.A. and Young, J.R. 2004. Calcareous nannoplankton evolution and diversity through time. In:

Thierstein, H.R. and Young, J.R. (Eds), Coccolithophores, 481–508. Springer; Berlin, Heidelberg.

Brinkhuis, H. 1994. Late Eocene to Early Oligocene dinoflagellate cysts from the Priabonian type-area (Northeast Italy): biostratigraphy and paleoenvironmental interpretation. *Palaeogeography*, *Palaeoclimatology*, *Palaeoecology*, **107**, 121–163.

Brönnimann, P. and Whittaker, J.E. 1983. A lectotype for Deuterammina (Deuterammina) rotaliformis (Heron-Allen and Earland) and new trochamminids from E. Ireland (Protozoa: Foraminiferida). *Bulletin of the British Museum of Natural History (Zoology)*, **45** (7), 347–358.

Brotzen, F. 1936. Foraminiferen aus dem schwedischen untersten Senon von Eriksdal in Schonen. *Sveriges Geologiska Undersökning ser. C*, **30** (3), 1–206.

Brotzen, F. 1940. Geology of the Flint Channel and Trindel Channel (Öresund). *Sveriges Geologiska Undersökning ser. C.*, **34** (5), 1–33. [In Swedish]

Brotzen, F. 1942. Die Foraminiferengattung *Gavelinella* nov. gen. und die Systematik der Rotaliiformes. *Sveriges Geologiska Undersökning ser. C*, **36** (8), 1–60.

Caron, M. and Homewood, P. 1983. Evolution of early planktic foraminifers. *Marine Micropaleontology*, **7**, 453–462.

Chaplot, V. and Mutema, M. 2021. Sources and main controls of dissolved organic and inorganic carbon in river basins: A worldwide meta-analysis. *Journal of Hydrology*, **603**, 126941.

Christensen, W.K. 1990. Upper Cretaceous belemnite stratigraphy of Europe. *Cretaceous Research*, **11**, 371–386.

Ciurej, A. 2023. *Stomiosphaerina bakae* sp. nov., a new calcareous dinocyst of the Upper Cretaceous of the Central European Basin. Plos One, 18 (10), e0292531.

Ciurej, A., Bąk, K. and Bąk, M. 2017. Late Albian calcareous dinocysts and calcitarchs record linked to environmental changes during the final phase of OAE 1d – a case study from the Tatra Mountains, Central Western Carpathians. *Geological Quarterly*, **61**, 887–895.

Ciurej, A., Dubicka, Z. and Poberezhskyy, A. 2023. Calcareous dinoflagellate blooms during the Late Cretaceous 'greenhouse' world – a case study from western Ukraine. *PeerJ*, **11**, e16201.

Cooper, L.W., Magen, C. and Grebmeier, J.M. 2022. Changes in the oxygen isotope composition of the Bering Sea contribution to the Arctic Ocean are an independent measure of increasing freshwater fluxes through the Bering Strait. *PlosOne*, **17**, e0273065.

Cushman, J.A. 1927a. Some new genera of the Foraminifera. *Contributions from the Cushman laboratory for foraminiferal research*, **2**, 77–81.

Cushman, J.A. 1927b. An outline of a reclassification of the foraminifera. *Contributions from the Cushman laboratory for foraminiferal research*, **3**, 1–105.

Davey, R.J., Williams, G.L., Downie, C. and Sarjeant, W.A.S.

1966. The genus *Hystrichosphaeridium* and its allies. *Studies on Mesozoic and Cainozoic dinoflagellate cysts*, **3**, 53–106.

Deflandre, G. and Cookson, I.C. 1955. Fossil microplankton from Australian Late Mesozoic and Tertiary sediments. *Australian Journal of Marine and Freshwater Research*, **6**, 242–313.

Delage, Y. and Hérouard, E. 1896. Traité de Zoologie Concrète Traité de Zoologie Concrète. Tome 1. La Cellule et Les Protozoaires, 584 pp. Schleicher Frères; Paris.

Dubicka, Z. 2015. Benthic foraminiferal biostratigraphy of the lower and middle Campanian of the Polish Lowlands and its application for interregional correlation. *Cretaceous Research*, **56**, 491–503.

Dubicka, Z. 2019. Chamber arrangement versus wall structure in the high-rank phylogenetic classification of Foraminifera. *Acta Palaeontologica Polonica*, **64**, 1–18.

Dubicka, Z. and Peryt, D. 2012. Latest Campanian and Maastrichtian palaeoenvironmental changes: implications from an epicontinental sea (SE Poland and western Ukraine). *Cretaceous Research*, **37**, 272–284.

Dubicka, Z., Peryt, D. and Szuszkiewicz, M. 2014. Foraminiferal evidence for paleogeographic and paleoenvironmental changes across the Coniacian–Santonian boundary in western Ukraine. *Palaeogeography, Palaeoclimatology, Palaeoecology*, **401**, 43–56.

Dubicka, Z., Wierzbowski, H. and Wierny, W. 2018. Oxygen and carbon isotope records of Upper Cretaceous foraminifera from Poland: vital and microhabitat effects. *Palaeogeography, Palaeoclimatology, Palaeoecology*, **500**, 33–51.

Ehrenberg, C.G. 1840. Uber die Bildung der Kreidenfelsen und des Kreidemergels durch unsichtbare Organismen. *Physikalische Abhandlungen der Königlischen Akademie der Wissenschaften zu Berlin*, **1838**, 59–147.

Eisenack, A. and Kjellström, G. 1972. Katalog der Fossilen Dinoflagellaten, Hystrichosphären und Verwandten Mikrofossilien. Band II. Dinoflagellaten, 1132 pp. E. Schweizerbart'sche Verlagsbuchhandlung; Stuttgart.

Fensome, R.A., Williams, G.L., Wood, S.E. and Riding, J.B. 2019. A review of the areoligeracean dinoflagellate cyst *Cyclonephelium* and morphologically similar genera. *Palynology*, **43**, 1–71.

Friedrich, O. 2010. Benthic foraminifera and their role to decipher paleoenvironment during mid-Cretaceous Oceanic Anoxic Events – the "anoxic benthic foraminifera" paradox. *Revue de Micropaléontologie*, **53**, 175–192.

Gale, A.S., Smith, A.B., Monks, N.E.A., Young, J.A., Howard, A., Wray, D.S. and Huggett, J.M. 2000. Marine biodiversity through the Late Cenomanian–Early Turonian: palaeoceanographic controls and sequence stratigraphic biases. *Journal of the Geological Society*, **157**, 745–757.

Gale, A.S., Voigt, S., Sageman, B.B. and Kennedy, W.J. 2008. Eustatic sea-level record for the Cenomanian (Late Cretaceous) – extension to the Western Interior Basin, USA. *Geology*, **36**, 859–862.

Hagenow, K.F. von. 1842. Monograph of the Cretaceous Fossils of Rügen. III Section: Molluscs. *Neues Jahrbuch für Mineralogie, Geognosie, Geologie und Petrefaktenkunde*, **1842**, 528–575.

Hallam, A. 1992. Controversies in modern geology: Evolution of geological theories in sedimentology, earth history and tectonics. *Earth Science Reviews*, **32**, 199–200.

Hancock, J.M. 1975. The sequence of facies in the Upper Cretaceous of northern Europe compared with that in the Western Interior. In: Caldwell, W.G.E. (Ed.), The Cretaceous System in the Western Interior of North America. *Geological Association of Canada, Special Paper*, **13**, 83–118.

Hancock, J.M. 1989. Sea-level changes in the British region during the Late Cretaceous. *Proceedings of the Geologists' Association*, **100**, 565–594.

Hancock, J.M. 1993. Transatlantic correlations in the Campanian–Maastrichtian stages by eustatic changes of sea-level. *Geological Society London, Special Publications*, **70**, 241–256.

Hancock, J.M. and Kauffman, E.G. 1979. The great transgressions of the Late Cretaceous. *Journal of the Geological Society*, **136**, 175–186.

Hardy, M.J. and Wrenn, J.H. 2009. Palynomorph distribution in modern tropical deltaic and shelf sediments – Mahakam Delta, Borneo, Indonesia. *Palynology*, **33**, 19–42.

Harland, R. 1988. Dinoflagellates, their cysts and Quaternary stratigraphy. *New Phytologist*, **108**, 111–120.

Hart, M.B. and Bailey, H.W. 1979. The distribution of planktonic Foraminiferida in the mid-Cretaceous of NW Europe. In: Wiedmann, J. (Ed.), Aspekte der Kriede Europas. *International Union of Geological Sciences*, *Series A*, **6**, 527–542.

Hildebrand-Habel, T. and Streng, M. 2003. Calcareous dinoflagellate associations and Maastrichtian–Tertiary climatic change in a high-latitude core (ODP Hole 689B, Maud Rise, Weddell Sea). *Palaeogeography, Palaeoclimatology, Palaeoecology*, **197**, 293–321.

Hofker, J. 1953. Types of Genera Described in Part III of the "Siboga Foraminifera". *The Micropaleontologist*, **7**, 26–28.

Jansonius, J. 1986. Re-examination of Mesozoic Canadian dinoflagellate cysts published by S.A.J. Pocock (1962, 1972). *Palynology*, **10**, 201–223.

Jorissen, F.J., de Stigter, H.C. and Widmark, J.G. 1995. A conceptual model explaining benthic foraminiferal microhabitats. *Marine Micropaleontology*, **26**, 3–15.

Kaiho, K. 1991. Global changes of Paleogene aerobic/anaerobic benthic foraminifera and deep-sea circulation. *Palaeogeography, Palaeoclimatology, Palaeoecology*, **83**, 65–85.

Kamptner, E. 1956. *Thoracosphaera deflandrei* nov. spec., ein bemerkenswertes Kalkflagellaten-Gehäuse aus dem Eocän

von Donzacq (Dep. Landes, Frankreich). *Österreichische Botanische Zeitschrift*, **103**, 448–456.

Kaplan, U. 2004. Neue Beobachtungen zu den Stromberg-Schichten, Untercampan, Oberkreide, südöstliches Münsterland. *Geologie und Paläontologie in Westfalen*, **62**, 71–110.

Kennedy, W.J. 1970. Trace fossils in the chalk environment. In: Crimes, T.P. and Harper, J.C. (Eds), Trace Fossils. *Geological Journal, Special Issue*, **3**, 263–281.

Keupp, H. 1982. Die Kalkigen Dinoflagellaten-Zysten des späten Apt und frühen Alb in Nordwestdeutschland. *Geologische Jahresberichte*, **65**, 307–363.

Keupp, H. 1987. Die kalkigen Dinoflagellatenzysten des Mittelalb bis Untercenoman von Escalles/Boulonnais (N-Frankreich). *Facies*, **16**, 37–88.

Keupp, H. 1993. Kalkige Dinoflagellaten-Zysten in Hell-Dunkel-Rhythmen des Ober-Hauterive/Unter-Barrême NW-Deutschlands. *Zitteliana*, **20**, 25–39.

Keupp, H. and Mutterlose, J. 1984. Organismenverteilung in den D-Beds von Speeton (Unterkreide, England) unter besonderer Berücksichtigung der kalkigen Dinoflagellaten-Zysten. *Facies*, **10**, 153–178.

Kienel, U. 1994. Die Entwicklung der kalkigen Nannofossilien und der kalkigen Dinoflagellaten-Zysten an der Kreide/Tertiär-Grenze in Westbrandenburg im Vergleich mit Profilen in Nordjutland und Seeland (Dänemark). *Berliner Geowissenschaftliche Abhandlungen*, **12**, 1–87.

Kirsch, K.H. 1991. Dinoflagellatenzysten aus der Oberkreide des Helvetikums und Nordultrahelvetikums von Oberbayern. *Münchner Geowissenschaftliche Abhandlungen, Reihe A, Geologie und Paläontologie*, **22**, 1–306.

Kohring, R. 1993. Kalkdinoflagellaten aus dem Mittel- und Obereozän von Jütland (Dänemark) und dem Pariser Becken (Frankreich) im Vergleich mit anderen Tertiär-Vorkommen. *Berliner Geowissenschaftliche Abhandlungen, Reihe E*, **6**, 1–164.

Korchagin, V.I. 1982. Systematics of the Globotruncanids. *Biulletin Moskovskogo Obshchestva Ispytateley Prirody, Otdel Geologicheskiy*, **57**, 114–121. [In Russian]

Kwon, E. Y., DeVries, T., Galbraith, E. D., Hwang, J., Kim, G. and Timmermann, A. 2021. Stable carbon isotopes suggest large terrestrial carbon inputs to the global ocean. *Global Biogeochemical Cycles*, **35**, e2020GB006684.

Lalicker, C.G. 1948. A new genus of Foraminifera from the Upper Cretaceous. *Journal of Paleontology*, **22**, 624.

Lasseur, E., Guillocheau, F., Robin, C., Hanot, F., Vaslet, D., Coueffe, R. and Neraudeau, D. 2009. A relative water-depth model for the Normandy Chalk (Cenomanian–Middle Coniacian, Paris Basin, France) based on facies patterns of metre-scale cycles. *Sedimentary Geology*, **213**, 1–26.

Leckie, R.M. 1987. Paleoecology of mid-Cretaceous planktonic foraminifera: a comparison of open ocean and epicontinental sea assemblages. *Micropaleontology*, **33**, 164–176.

Lentin, J.K. and Williams, G.L. 1985. Fossil dinoflagellates: index to genera and species, 1985 edition. *Canadian Technical Report of Hydrography and Ocean Sciences*, **60**, 1–451.

Lentin, J.K. and Williams, G.L. 1993. Fossil dinoflagellates: index to genera and species, 1993 edition, 856 pp. American Association of Stratigraphic Palynologists; Houston.

Leszczyński, K. 2010. Lithofacies evolution of the Late Cretaceous basin in the Polish Lowlands. *Biuletyn Państwowego Instytutu Geologicznego*, **443**, 33–54.

Leszczyński, K. 2012. The internal geometry and lithofacies pattern of the Upper Cretaceous–Danian sequence in the Polish Lowlands. *Geological Quarterly*, **56**, 363–386.

Linnert, C., Mutterlose, J. and Erbacher, J. 2010. Calcareous nannofossils of the Cenomanian/Turonian boundary interval from the Boreal Realm (Wunstorf, northwest Germany). *Marine Micropaleontology*, **74**, 38–58.

Longoria, J.F. 1974. Stratigraphic, morphologic and taxonomic studies of Aptian planktonic foraminifera. *Revista Española de Micropaleontología*, **Numero Extraordinario**, 5–107.

Machalski, M. and Malchyk, O. 2019. Relative bathymetric position of opoka and chalk in the Late Cretaceous European Basin. *Cretaceous Research*, **102**, 30–36.

Marie, P. 1941. Les Foraminifères de la craie à *Belemnitella mucronata* du Bassin de Paris, 296 pp. Mémoires du Muséum National d'Histoire Naturelle de Paris, Nouvelle Série; Paris.

Marsson, T. 1878. Die Foraminiferen der weissen Schreibkreide der Insel Rügen. *Mitteilungen aus dem Naturwissenschaftlichen Verein für Neu-Vorpommern und Rügen in Greifswald*, **10**, 115–196.

Marwick, T.R., Tamooh, F., Teodoru, C.R., Borges, A.V., Darchambeau, F. and Bouillon, S. 2015. The age of river-transported carbon: A global perspective. *Global Biogeochemical Cycles*, **29**, 122–137.

Miller, K.G., Wright, J.D. and Browning, J.V. 2005. Visions of ice sheets in a greenhouse world. *Marine Geology*, **217**, 215–231.

Mushenko, A.I. 1961. Origin and structure of swells in the Russian Platform. *Izvestiya Akademii Nauk SSSR. Seriya Geologicheskaya*, **4**, 31–42. [In Russian]

Niebuhr, B. 1995. Fazies-Differenzierungen und ihre Steuerungsfaktoren in der höheren Oberkreide von S-Niedersachsen/Sachsen-Anhalt (N-Deutschland). *Berliner Geowissenschaftliche Abhandlungen, Reihe A*, **174**, 1–131.

Niebuhr, B. 1999. Cyclostratigraphic correlation of outcrops and electronic borehole measurements in Middle Campanian marl/limestone rhythmites of North Germany. *Beringeria*, **23**, 47–54.

Niebuhr, B. 2006. Multistratigraphische Gliederung der norddeutschen Schreibkreide (Coniac bis Maastricht), Korrelation von Aufschlussen und Bohrungen. Zeitschrift der deutschen Gesellschaft für Geowissenschaften, *Zeitschrift der Deutschen Gesellschaft für Geowissenschaften*, **157**, 245–261.

Niebuhr, B. and Reich, M. 2004. Exkursion 7: Das Campan (höhere Ober-Kreide) der Lehrter Westmulde bei Hannover. In: Reitner, J., Reich, M. and Schmidt, G. (Eds), Geobiologie 2, 74. Jahrestagung der Paläontologischen Gesellschaft in Göttingen 02. bis 08. Oktober 2004. Excursionen und Workshops, 193–210. Universitätsdrucke Göttingen; Göttingen.

Niebuhr, B., Volkmann, R. and Schönfeld, J. 1997. Das obercampane polyplocum-Event in der Lehrter Westmulde (Oberkreide, N-Deutschland): Bio-/Litho-/Sequenzstratigraphie, Faziesentwicklung und Korrelation. *Freiberger Forschungshefte*, **468**, 211–244.

Niechwedowicz, M., Walaszczyk, I. and Barski, M. 2021. Phytoplankton response to palaeoenvironmental changes across the Campanian–Maastrichtian (Upper Cretaceous) boundary interval of the Middle Vistula River section, central Poland. *Palaeogeography*, *Palaeoclimatology*, *Palaeoecology*, **577**, 110558.

Olde, K., Jarvis, I., Pearce, M., Walaszczyk, I. and Tocher, B. 2016. Organic-walled dinoflagellate cyst records from a prospective Turonian–Coniacian (Upper Cretaceous) GSSP, Słupia Nadbrzeżna, Poland. *Cretaceous Research*, **65**, 17–24.

Olfer'ev, A.G. and Alekseev, A.S. 2003. Biostratigraphic Zonation of the Upper Cretaceous in the East European Platform. *Stratigraphy and Geological Correlation*, **11**, 172–198.

Olfer'ev, A.G., Alekseev, A.S., Beniamovskii, V.N.,Vishnevskaya, V.S., Ivanov, A.V., Pervushov, E.M., Sel'tser, V.B., Kharitonov, V.M. and Shcherbinina, E.A. 2004. The Mezino-Lapshinovka reference section of the Upper Cretaceous and problems of Santonian–Campanian boundary in Saratov area near the Volga River. *Stratigraphy and Geological Correlation*, **12**, 603–636.

Orbigny, A. d' 1840. Mémoire sur les foraminiféres de la craie blanche du bassin de Paris. *Memoires de la Societe Geologique de France*, **4**, 1–51.

Parker, W.K. and Jones, T.R. 1859. On the nomenclature of the Foraminifera. II. On the species enumerated by Walker and Montagu. *Annals and Magazine of Natural History*, **4**, 333–351.

Pasternak, S.I. 1959. Biostratigraphy of the Cretaceous deposits of the Volyn-Podilsky Plate, 98 pp. Vydavnytstvo Akademii Nauk Ukrainskoi RSR; Kyiv. [In Ukrainian]

Pasternak, S.I., Gavrylyshyn, V.I., Gynda, V.A., Kociubyn'skyi, S.P. and Sen'kows'kyi, Y.M. 1968. Stratigraphy and fauna of Cretaceous Deposits in the Western Ukraine (excluding the Carpathians), 272 pp. Naukova Dumka; Kyiv. [In Ukrainian]

Pasternak, S.I., Sen'kows'kyi, Y.M. and Gavrylyshyn, V.I. 1987. Volyn-Podolia in the Cretaceous period, 258 pp. Naukova Dumka; Kyiv. [In Ukrainian]

Paustian, K., Larson, E., Kent, J., Marx, E. and Swan, A. 2019. Soil C Sequestration as a Biological Negative Emission Strategy. *Frontiers in Climate*, **1**, 8.

Pearce, M.A., Jarvis, I., Monkenbusch, J., Thibault, N., Ullmann, C.V. and Martinez, M. 2022. Coniacian–Campanian palynology, carbon isotopes and clay mineralogy of the Poigny borehole (Paris Basin) and its correlation in NW Europe. *Comptes Rendus Géoscience*, **354** (S3), 121.

Pessagno, E.A. 1967. Upper Cretaceous planktonic foraminifera from the western Gulf Coastal Plain. *Palaeontographica Americana*, **5**, 245–445.

Pflaumann, U. and Krasheninnikov, V.A. 1978. Cretaceous calcisphaerulids from DSDP Leg 41, eastern north Atlantic. *Initial Reports of the Deep-Sea Drilling Project*, **41**, 817–839.

Plummer, H.J. 1931. Some Cretaceous foraminifera in Texas. *University of Texas Bulletin*, **3101**, 109–203.

Powell, A.J., Lewis, J. and Dodge, J.D. 1992. The palynological expressions of post-Palaeogene upwelling: a review. *Geological Society, London, Special Publications*, **64**, 215–226.

Powell, A.J., Brinkhuis, H. and Bujak, J.P. 1996. Upper Paleocene–Lower Eocene dinoflagellate cyst sequence biostratigraphy of southeast England. *Geological Society, London, Special Publications*, **101**, 145–183.

Pożaryska, K. 1954. The Upper Cretaceous index foraminifers from central Poland. *Acta Geologica Polonica*, **4**, 241–276. [In Polish with English summary]

Pożaryski, W. 1948. Jurassic and Cretaceous between Radom, Zawichost and Kraśnik, Central Poland. *Biuletyn Instytutu Geologicznego*, **46**, 5–106. [In Polish with English summary]

Prauss, M. 2000. The oceanographic and climatic interpretation of marine palynomorph phytoplankton distribution from Mesozoic, Cenozoic and Recent sections. *Göttinger Arbeiten zur Geologie und Paläontologie*, **76**, 1–235.

Pross, J. 2001. Paleo-oxygenation in Tertiary epeiric seas: evidence from dinoflagellate cysts. *Palaeogeography, Palaeoclimatology, Palaeoecology*, **166**, 369–381.

Pross, J. and Brinkhuis, H. 2005. Organic-walled dinoflagellate cysts as paleoenvironmental indicators in the Paleogene; a synopsis of concepts. *Paläontologische Zeitschrift*, **79**, 53–59.

Puckett, T.M. 1991. Absolute paleobathymetry of Upper Cretaceous chalks based on ostracodes – Evidence from the Demopolis Chalk (Campanian and Maastrichtian) of the northern Gulf Coastal Plain. *Geology*, **19**, 449–452.

Radmacher, W. and Uchman, A. 2020. Oxygen as a factor controlling palynological record: an example from the Cenomanian–Turonian transition in the Rybie section, Polish Carpathians. *Marine and Petroleum Geology*, **112**, 104067.

Radmacher, W., Vasquez, O.J., Tzalam, M., Jolomná, M., Molineros, A. and Eldrett, J.S. 2021. What happened to the organic matter from the Upper Cretaceous succession in

Guatemala, Central America? *Marine and Petroleum Geology*, **133**, 105246.

Rebotim, A., Voelker, A. H. L., Jonkers, L., Waniek, J. J., Meggers, H., Schiebel, R., Fraile, I., Schulz, M. and Kucera, M. 2017. Factors controlling the depth habitat of planktonic foraminifera in the subtropical eastern North Atlantic. *Biogeosciences*, **14**, 827–859.

Reid, R.E.H. 1968. Bathymetric distributions of Calcarea and Hexactinellida in the present and the past. *Geological Magazine*, **105**, 546–559.

Reid, R.E.H. 1973. The chalk sea. *The Irish Naturalists' Journal*, **17**, 357–375.

Reuss, A.E. 1860. Die Foraminiferen der westphälischen Kreideformation. *Sitzungsberichte der Königlich-Kaiserlichen Akademie der Wissenschaften, Mathematisch-Naturwissenschaftliche Classe*, **40**, 147–238.

Roncaglia, L. and Kuijpers, A. 2006. Revision of the palynofacies model of Tyson (1993) based on recent high-latitude sediments from the North Atlantic. *Facies*, **52**, 19–39.

Savko, A.D. and Ivanova, E.O. 2009. Facies characteristics of the Upper Cretaceous deposits of the south-western part of the Voronezh Anticline. *Vestnik of the Voronezh State University, Series Geology*, **2**, 61–78. [In Russian]

Schiøler, P. and Wilson, G.J. 1993. Maastrichtian dinoflagellate zonation in the Dan Field, Danish North Sea. *Review of Palaeobotany and Palynology*, **78**, 221–351.

Schiøler, P., Crampton, J.S. and Laird, M.G. 2002. Palynofacies and sea-level changes in the middle Coniacian–late Campanian (Late Cretaceous) of the East Coast Basin, New Zealand. *Palaeogeography, Palaeoclimatology, Palaeoecology*, **188**, 101–125.

Schmiedl, G. 2019. Use of foraminifera in climate science. In: von Storch, H. (Ed.), Oxford Research Encyclopaedia of Climate Science, 1–51. Oxford University Press; Oxford.

Schmittner, A., Bostock, H.C., Cartapanis, O., Curry, W.B., Filipsson, H.L., Galbraith, E.D., Gottschalk, J., Herguera, J.C., Hoogakker, B., Jaccard, S.L., Lisiecki, L.E., Lund, D.C., Martínez-Méndez, G., Lynch-Stieglitz, J., Mackensen, A., Michel, E., Mix, A.C., Oppo, D.W., Peterson, C.D., Repschläger, J., Sikes, E.L., Spero, H.J. and Waelbroeck, C. 2017. Calibration of the carbon isotope composition (δ^{13}C) of benthic foraminifera. *Paleoceanography*, **32**, 512–530.

Scotese, C.R. 2014. Atlas of Late Cretaceous Maps, PALEOMAP Atlas for ArcGIS, volume 2, The Cretaceous, Maps 16–22, Mollweide Projection. PALEOMAP Project; Evanston, IL.

Skelton, P.W., Spicer, R.A., Kelley, S.P. and Gilmour, I. 2003. The Cretaceous World, 360 pp. Cambridge University Press; Cambridge.

Slimani, H. 2001. Les kystes de dinoflagellés du Campanien au Danien dans la région de Maastricht (Belgique, Pays-Bas) et de Turnhout (Belgique): biozonation et corrélation avec d'autres régions en Europe occidentale. *Geologica et Palaeontologica*, **35**, 161–201.

Slimani, H. 2003. A new genus and two new species of dinoflagellate cysts from the Upper Cretaceous of the Maastrichtian type area and Turnhout (northern Belgium). *Review of Palaeobotany and Palynology*, **126**, 267–277.

Sluijs, A., Pross, J. and Brinkhuis, H. 2005. From greenhouse to icehouse; organic-walled dinoflagellate cysts as paleoenvironmental indicators in the Paleogene. *Earth-Science Reviews*, **68**, 281–315.

Spero, H.J., Bijma, J., Lea, D.W. and Bemis, B.E. 1997. Effect of seawater carbonate concentration on foraminiferal carbon and oxygen isotopes. *Nature*, **390**, 497–500.

Streng, M., Hildebrand-Habel, T. and Willems, H. 2002. Revision of the genera *Sphaerodinella* Keupp and Versteegh, 1989 and *Orthopithonella* Keupp in Keupp and Mutterlose, 1984 (Calciodinelloideae, calcareous dinoflagellate cysts). *Journal of Paleontology*, **76**, 397–407.

Streng, M., Hildebrand-Habel, T. and Willems, H. 2004. Long-term evolution of calcareous dinoflagellate associations since the Late Cretaceous: comparison of a high-and a low-latitude core from the Indian Ocean. *Journal of Nannoplankton Research*, **26**, 13–45.

Streng, M., Basanova, M., Rehakova, S. and Willems, H. 2009. An exceptional flora of calcareous dinoflagellates from the middle Miocene of the Vienna Basin, SW Slovakia. *Review of Palaeobotany and Palynology*, **153**, 225–244.

Subbotina, N.N. 1959. Planktonic foraminifera. In: Rauzer-Chernousova, D.M. and Fursenko, A.V. (Eds), Principles of paleontology, part 1, Protozoa, 1–368. Akademia Nauk SSSR; Moscow.

Surlyk, F., Rasmussen, S.L., Boussaha, M., Schiøler, P., Schovsbo, N.H., Sheldon, E., Stemmerik, L. and Thibault, N. 2013. Upper Campanian–Maastrichtian holostratigraphy of the eastern Danish Basin. *Cretaceous Research*, **46**, 232–256.

Thalmann, H.E. 1939. Bibliography and index to new genera, species and varieties of foraminifera for the year 1936. *Journal of Paleontology*, **13**, 425–465.

Tyson, R.V. 1993. Palynofacies Analysis. In: Jenkins, D.G. (Ed.), Applied Micropalaeontology, 153–191. Springer; Dordrecht.

Tyson, R.V. 1995. Abundance of Organic Matter in Sediments: TOC, Hydrodynamic Equivalence, Dilution and Flux Effects. In: Tyson, R.V. (Ed.), Sedimentary Organic Matter, 81–118. Springer; Dordrecht.

Young, J.R., Bergen, J.A, Bown, P.R., Burnett, J.A., Fiorentino, A., Jordan, R.W., Kleijne, A., van Niel, B.E., Ton Romein A.J. and Von Salis, K. 1997. Guidelines for coccolith and calcareous nannofossil terminology. *Palaeontology*, **40**, 875–912.

Van der Zwaan, G.J., Duijnstee, A.I., Den Dulk, M., Ernst, S.R., Jannink, N.T. and Kouwenhoven, T.J. 1999. Benthic foraminifers: proxies or problems?: a review of paleoecological concepts. *Earth-Science Reviews*, **46**, 213–236.

Vasilenko, V.P. 1961. Upper Cretaceous foraminifera of the

Mangyshlak Peninsula. *Proceedings of the Oil Research Geological Institute (VNIGRI)*, **171**, 1–487. [In Russian]

Vejbæk, O.V. and Andersen, C. 2002. Post mid-Cretaceous inversion tectonics in the Danish Central Graben – regionally synchronous tectonic events. *Bulletin of the Geological Society of Denmark*, **49**, 129–144.

de Vernal, A., Radi, T., Zaragosi, S., Van Nieuwenhove, N., Rochon, A., Allan, E., De Schepper, S., Eynaud, F., Head, M.J., Limoges, A. and Londeix, L. 2020. Distribution of common modern dinoflagellate cyst taxa in surface sediments of the Northern Hemisphere in relation to environmental parameters: The new n=1968 database. *Marine Micropaleontology*, **159**, 101796.

Vogler, J. 1941. Ober-Jura und Kreide von Misol. In: Boehm, G. and Wanner, J. (Eds), Beitrage zur Geologie von Niederlandisch-Indian, 243–293. Schweizerbart; Stuttgart.

Voigt, T., Kley, J. and Voigt, S. 2021. Dawn and dusk of Late Cretaceous basin inversion in central Europe. *Solid Earth*, **12**, 443–471.

Walaszczyk, I. 1997. Biostratigraphie und Inoceramen des oberen Unter-Campan und unteren Ober-Campan Norddeutchlands. *Geologie und Paläontologie in Westfalen*, **49**, 1–111.

Walaszczyk, I., Cobban, W.A., Wood, C.J. and Kin, A. 2008. The '*Inoceramus*' *azerbaydjanensis* fauna (Bivalvia) and its value for chronostratigraphic calibration of the European Campanian (Upper Cretaceous). *Bulletin de l'Institut Royal des Sciences Naturelles de Belgique*, **78**, 229–238.

Walaszczyk, I., Dubicka, Z., Olszewska-Nejbert, D. and Remin, Z. 2016. Integrated biostratigraphy of the Santonian through Maastrichtian (Upper Cretaceous) of extra-Carpathian Poland. *Acta Geologica Polonica*, **66**, 313–350.

Walaszczyk, I. and Remin, Z. 2015. Kreda obrzeżenia Gór Świętokrzyskich. 84 Zjazd Polskiego Towarzystwa Geologicznego, Chęciny, 9–11 września, 2015, 41–50.

Wall, D., Dale, B., Lohmann, G.P. and Smith, W.K. 1977. The environmental and climatic distribution of dinoflagellate cysts in modern marine sediments from regions in the North and South Atlantic Oceans and adjacent seas. *Marine Micropaleontology*, **2**, 121–200.

Wendler, J. and Willems, H. 2002. Distribution pattern of calcareous dinoflagellate cysts across the Cretaceous–Tertiary boundary (Fish Clay, Stevns Klint, Denmark): Implications for our understanding of species-selective extinction. In: Koebarl, C. and MacLeod, K.G. (Eds), Catastrophic events and mass extinctions: impacts and beyond. *Geological Society of America, Special Papers*, **356**, 265–276.

Wendler, I., Huber, B.T., MacLeod, K.G. and Wendler, J.E. 2013. Stable oxygen and carbon isotope systematics of exquisitely preserved Turonian foraminifera from Tanzania – Understanding isotopic signatures in fossils. *Marine Micropaleontology*, **102**, 1–33.

White, H.H. 1842. On fossil Xanthidia. *Microscopical Journal, London*, **11**, 35–40.

Wiese, F., Zobel, K. and Keupp, H. 2015. Calcareous dinoflagellate cysts and the Turonian nutrient crisis – data from the upper Turonian of the Lower Saxony Basin (northern Germany). *Cretaceous Research*, **56**, 673–688.

Wiese, F., Zobel, K. and Mortimore, R.N. 2018. Intrinsic processes control late Turonian calcareous dinoflagellate cyst assemblages – A case study from the Sussex chalk (England). *Cretaceous Research*, **87**, 206–217.

Zonneveld, K.A., Marret, F., Versteegh, G.J., Bogus, K., Bonnet, S., Bouimetarhan, I., Crouch, E., de Vernal, A., Elshanawany, R., Edwards, L. and Esper, O. 2013. Atlas of modern dinoflagellate cyst distribution based on 2405 data points. *Review of Palaeobotany and Palynology*, **191**, 1–197.

Zonneveld, K.A., Versteegh, G. and Kodrans-Nsiah, M. 2008. Preservation and organic chemistry of Late Cenozoic organic-walled dinoflagellate cysts: a review. *Marine Micropaleontology*, **68**, 179–197.

Zonneveld, K.A., Versteegh, G.J. and de Lange, G.J. 1997. Preservation of organic-walled dinoflagellate cysts in different oxygen regimes: a 10,000 year natural experiment. *Marine Micropaleontology*, **29**, 393–405.

APPENDIX 1

			Sample number	planktonic				benthic																			Total number
				Globigerinelloididae	Rugoglobigerinidae	Globotruncanidae	Planoheterohelix	Arenobulinina	Ataxophragmium	Bolivina incrassata	Cibicidoides voltzianus	Gavelinella annae	Gavelinella monterelensis	Gavelinella pertusa	Globorotalites sp.	Gyroidinoides sp.	Lagenida sp.	Lenticulina sp.	Loxostomum eleyi	Osangularia sp.	Plectina sp.	Praebulimina sp.	Pullenia sp.	Spiroplectammina sp.	Stensioeina pommerana	Trochammina sp.	Valvulinella sp.	
MIDDLE CAMPANIAN	Globorotalites emdyensis	'Inoceramus' azerbaydjanensis–'I.' vorhelmensis	15	49	11	1	2	5	0	0	18	2	9	24	52	8	8	0	0	7	1	6	3	0	38	3	3	250
			14	11	9	1	1	6	7	0	21	6	13	23	26	54	1	2	2	9	1	15	2	0	35	3	2	250
			13	7	14	6	2	38	0	0	29	11	11	24	28	37	5	4	0	3	8	2	2	0	17	2	0	250
			12	35	8	28	1	5	4	0	19	3	7	22	22	28	4	2	0	7	0	8	0	0	39	4	4	250
			11	20	10	7	1	11	2	0	23	10	11	31	39	34	3	3	4	4	2	4	0	0	29	2	0	250
			10	2	4	8	1	21	0	0	16	4	11	23	89	8	11	5	0	16	1	3	0	0	24	3	0	250
			9	47	11	7	41	5	0	0	14	6	16	17	20	10	10	2	0	11	0	2	1	0	29	1	0	250
			8	15	11	1	1	10	6	0	21	9	13	27	14	26	3	2	1	28	1	14	0	0	45	0	2	250
			7	26	26	2	1	9	0	0	25	7	14	12	57	6	6	3	0	14	0	11	4	0	24	2	1	250
	Gavelinella annae		6	44	22	1	1	8	3	0	20	8	15	16	29	5	4	6	1	7	4	9	0	0	45	0	2	250
			5	33	46	0	1	6	0	0	15	5	4	12	19	16	3	2	17	14	1	20	1	0	35	0	0	250
			1/0	12	22	5	1	10	1	1	22	4	12	9	49	5	9	2	0	25	2	2	1	0	52	3	1	250
			2	15	30	6	1	7	0	0	26	3	6	13	45	7	10	0	0	14	2	4	4	1	52	2	2	250
			3	41	23	4	1	6	2	0	16	14	8	17	28	26	3	3	1	8	0	7	1	0	36	3	2	250
			4	15	8	21	1	4	4	0	23	10	12	16	64	13	11	4	1	15	0	0	1	0	27	0	0	250

Table A1. Distribution of planktonic and benthic foraminifera in the Belgorod succession.

			Sample number	planktonic			
				Globigerinelloidida	Rugoglobigerinidae	Globotruncanidae	Total number
MIDDLE CAMPANIAN	Globorotalites emdyensis	'Inoceramus' azerbaydjanensis–'I.' vorhelmensis	15	119	30	1	150
			14	80	63	7	150
			13	28	93	29	150
			12	68	17	65	150
			11	66	24	60	150
			10	40	74	36	150
			9	106	33	11	150
			8	90	34	26	150
			7	73	75	2	150
	Gavelinella annae		6	82	60	8	150
			5	70	75	5	150
			1/0	49	93	8	150
			2	65	63	22	150
			3	88	29	33	150
			4	57	49	44	150

Table A2. Distribution of planktonic foraminifera in the Belgorod succession, with a maximum foraminiferal count of 150.